Tomato yellow leaf curl virus V2 protein plays a critical role in the nuclear export of V1 protein and viral systemic infection

Wenhao Zhao[1, 2], Yinghua Ji[1], Shuhua Wu[1], Elizabeth Barton[2], Yongjian Fan[1], Xiaofeng Wang[2]*, Yijun Zhou[1]*

[1]Institute of Plant Protection, Jiangsu Academy of Agricultural Sciences, Key Lab of Food Quality and Safety of Jiangsu Province—State Key Laboratory Breeding Base, Nanjing, 210014, China

[2]School of Plant and Environmental Sciences, Virginia Tech, Blacksburg, VA, 24061, United States of America

*Corresponding author: Yijun Zhou: yjzhou@jaas.ac.cn

Xiaofeng Wang: reachxw@vt.edu

Abstract

Geminiviruses are an important group of circular, single-stranded DNA viruses that cause devastating diseases in crops. Geminiviruses replicate their genomic DNA in the nucleus. The newly-synthesized viral DNA is subsequently transported to the cytoplasm, moved to adjacent cells through plasmodesmata with the help of viral movement proteins, and, ultimately, moved long-distance to establish systemic infection. Thus, the nucleocytoplasmic transportation is crucial for a successful

infection by geminiviruses. For *Tomato yellow leaf curl virus* (TYLCV), the V1 protein is known to bind and shuttle viral genomic DNA, but the role of V2 protein in this process is still unclear. Here, we report that the nucleus-localized V1 protein dramatically decreases when co-expressed with V2 protein, and that V2-facilitated nuclear export of V1 protein depends on host exportin-α and a specific V1-V2 interaction. Chemical inhibition of exportin-α or a substitutions at cysteine 85 of V2 protein, which abolishes the V1-V2 interaction, blocks the promoted redistribution of V1 protein to the perinuclear region and the cytoplasm. When the $V2^{C85S}$ mutation is incorporated into a TYLCV infectious clone, the TYLCV-C85S causes delayed onset of very mild symptoms compared to wild-type TYLCV, indicating that the V1-V2 interaction and, thus, V2-mediated nuclear export of V1 protein is crucial for viral spread and systemic infection. Our data point to a critical role of the V2 protein in promoting the nuclear export of the V1 protein, likely by promoting V1-mediated nucleocytoplasmic transportation of TYLCV genomic DNA, and in turn, promoting viral systemic infection.

Author summary

As both replication and the transcription of geminiviruses occur in the nucleus, transportation of the viral genomic DNA into and out of the nucleus of the infected cells is essential for a successful infection cycle. However, the nuclear export of geminiviruses is still little known and even less is known about the process for

43 monopartite geminiviruses. We use TYLCV, a typical monopartite begomovirus in
44 the family *Geminiviridae*, to examine the nucleocytoplasmic transportation. In this
45 study, we found TYLCV V2 is able to redistribute the nucleus-localized V1 protein to
46 the perinuclear region. Moreover, the nuclear export of V1 protein is dependent on the
47 V1-V2 interaction and host exportin-α. Blocking the V1-V2 interaction impeded the
48 V2-mediated V1 protein redistribution and decrease TYLCV infection efficiency with
49 delayed and mild symptoms. This report shows us a new explanation for the role of
50 V2 in the nuclear export of V1 protein and TYLCV viral systemic infection.
51

52 ## Introduction

53 Geminiviruses are a group of plant viruses with a circular, single-stranded DNA
54 genome. Viruses in this family cause devastating diseases in crop plants, leading to
55 agricultural losses worldwide [1-4]. While viral gene expression occurs in the
56 cytoplasm, replication of geminiviruses occurs in the nucleus of infected host cells [5].
57 It is crucial that viral proteins involved in replication enter into the nucleus to execute
58 their functions and in addition, newly synthesized viral genomic DNA are exported
59 from the nucleus to the cytoplasm for further spread to adjacent cells and cause
60 systemic infection through long-distance movement. Therefore, the
61 nucleocytoplasmic shuttling of geminiviruses proteins and genomic DNA is of great
62 significance for viral systemic infection and virus control.

Geminiviruses can be divided into two major groups based on their genomic components: one group is the monopartite geminiviruses, while the other group is the bipartite geminiviruses [5]. The bipartite geminiviruses genome is composed of two circular 2.5- to 2.8-kb ss-DNA molecules (DNA-A and DNA-B). The movement of bipartite geminiviruses requires two proteins, BV1 and BC1, that are encoded by DNA-B [6-10]. BV1 is a nuclear shuttle protein and plays an important role in the nucleocytoplasmic shuttling of viral genomic DNA [6-9, 11]. BC1 facilitates cell-to-cell movement after genomic DNAs are exported out of the nucleus.

The genome of monopartite geminiviruses contains only one component, DNA-A. Because monopartite geminiviruses lack the DNA-B component, the mechanism for movement of the virus is not clear yet. As DNA-A encode more viral proteins compared with DNA-B, and many of the proteins are multifunctional, which makes it more challenging to examine the nucleocytoplasmic shuttling of viral DNA of monopartite geminiviruses. Only a few viruses have been examined, such as *Maize streak virus* (MSV) and *Tomato yellow leaf curl virus* (TYLCV) [12, 13, 14]. It has been reported that V1 protein binds to viral genomic DNA and shuttles them between the nucleus and cytoplasm [11, 15, 16]. It was later reported that host proteins are also required for the process. Nuclear transporter KAPα helps TYLCV to enter the nucleus [17, 18] and exportin-α is required for the nuclear export of the C4 protein of *Tomato leaf curl Yunnan virus* (TLCYnV) [19]. In addition, nuclear shuttling of monopartite geminiviruses also involve viral proteins other than V1 protein,

84 suggesting a protein complex may be involved [13, 19, 20]. However, it is unclear
85 what viral proteins or how they work together to accomplish transportation between
86 the nucleus and the cytoplasm.

87 TYLCV is a typical monopartite begomovirus in the family *Geminiviridae*. The
88 single ssDNA genome has six open reading frames (ORFs) and an intergenic region
89 (IR). Four ORFs (C1, C2, C3 and C4) are located on the complementary strand and
90 the other two ORFs (V1 and V2) are located on the viral strand [21].
91 Replication-associated protein (Rep) encoded by C1, transcriptional activator protein
92 (TrAP) encoded by C2 and replication enhancer protein (REn) encoded by C3 are all
93 involved in viral replication. C4 protein is likely involved in symptom development
94 and viral movement. V1 encodes the capsid protein (CP), which facilitates virion
95 assembly and viral trafficking [1, 13, 22, 23]. V2 protein is a gene silencing
96 suppressor at both the post-transcriptional stage (PTGS) [24] and the transcriptional
97 level stage (TGS) [25]. V2 protein is also involved in the regulation of host defense
98 responses [26] and viral movement [13], playing important roles in viral spread and
99 systemic infection [27].

100 For the nucleocytoplasmic transportation of TYLCV, V1 protein is well-known
101 as a nuclear shuttle protein and for its role in binding viral genomic DNA [13]. Early
102 studies showed that V1 protein binds viral genomic ssDNA in the cytoplasm and
103 moves them into the nucleus for replication [28, 29]. V1 protein also interacts with the
104 host plant nuclear transporter protein to facilitate the entry of virus into the nucleus

105 [17]. In addition, V1 protein also helps viral genomic DNA to move out of the
106 nucleus for further translation and expression when offspring genomic DNA is
107 synthesized [13]. This suggests that V1 protein is functionally equivalent to BV1 of
108 bipartite geminiviruses. However, several lines of evidence suggest that other viral
109 proteins, such as V2, are also involved [5, 13, 17, 30, 31, 32]. Rojas et al. found that
110 the efficiency of nuclear export of viral DNA was enhanced by 20-30% in the
111 presence of V2 protein, suggesting a role for V2 protein in the V1 protein-mediated
112 nuclear export of viral genomic DNA [13]. However, the mechanism whereby V2
113 protein facilitates V1-mediated viral genomic DNA trafficking from the nucleus is
114 unknown.

115 In this study, we demonstrate that V2 protein affects the subcellular localization
116 of V1 protein by dramatically decreasing the nucleus-localized V1 protein in
117 *Nicotiana benthamian* cells, possibly through host exportin-α (XPO I), which often
118 mediates nuclear export of proteins. A specific interaction between V2 and V1
119 proteins has been identified by co-immunoprecipitation (Co-IP) and bimolecular
120 fluorescence complementation (BiFC). Substitutions in cystine 85 of the V2 protein
121 inhibits the V1-V2 interaction, blocks the effect of V2 protein on the subcellular
122 localization of V1 protein, and causes delayed and mild symptom in plants. Our
123 results indicate that V2 protein interacts with V1 protein, promotes the nuclear export
124 of V1 protein, and plays an important role in viral systemic infection.
125

Results

V2 Protein Affects the Nuclear Localization of V1 Protein

TYLCV V1 protein is known as a nucleocytoplasmic shuttle protein that facilitates the transport of viral genomic DNA into and out of the nucleus. When expressed in cells of *Nicotiana benthamiana* by agroinfiltration as a YFP-tagged protein, V1-YFP, the YFP signal was found in both the nucleus and cytoplasm at 40 hours post infiltration (hpi) (Fig 1a), consistent with its role in nuclear transportation of viral genomic DNA.

Since V2 protein was reported to facilitate the export of viral genomic DNA from the nucleus [13], we tested whether V2 protein does so by promoting the nucleus export of the V1 protein. We first tested for the subcellular localization of V2 as a YFP-tag (V2-YFP) in *N. benthamiana* cells via agroinfiltration. The fluorescence signal was observed under a laser confocal microscope at 40 hpi. YFP-V2 was mainly present in the cytoplasm and perinuclear regions, but a much weaker signal was also present in the nucleus (Fig 1b). To further clarify the function of V2 protein in the nuclear export of TYLCV, we co-expressed FLAG-tagged V2 protein (FLAG-V2) with V1-YFP. Interestingly, only a weaker fluorescence signal of V1 protein was found in the nucleus compared to that of V1 protein alone (Fig 1a). To rule out the possibility that the weaker signal of V1-YFP in the nucleus was due to decreased expression and/or stability in the presence of V2, we checked the accumulation of V1-YFP by Western blotting. Our results showed that both V2 and V1 proteins were

147 expressed well when co-expressed (Fig 1a). An increased accumulation of V1-YFP
148 was sometimes noticed when it was co-expressed with FLAG-V2 than when it was
149 expressed alone, indicating that the lower V1-YFP signal in the nucleus was not due
150 to its decreased accumulation in the presence of FLAG-V2.

151 To confirm our visual observations, we performed a fractionation assay to
152 separate the nucleus from the cytoplasm [19] and tested the localization of V1-YFP in
153 the absence and presence of the V2 protein. To this end, we expressed FLAG-V2 and
154 V1-YFP in Histone 2B (H2B)-RFP transgenic plants. As shown in Fig 1c, we only
155 detected H2B-RFP in the nuclear fraction but not the cytoplasmic fraction; a
156 cytoplasmic marker, phosphoenolpyruvate carboxylase (PEPC), was only present in
157 the cytoplasm fraction, not in the nuclear fraction. Under such conditions, FLAG-V2
158 was primarily detected in the cytoplasm fraction but only weakly in the nucleus.
159 Although V1-YFP was detected in both fractions when expressed alone, the amount
160 in the nuclear fraction significantly decreased in the presence of FLAG-V2, which is
161 consistent with the results based on fluorescence microscopy (Fig 1c). To provide a
162 numeric reading, we set the sum of V1-YFP signal intensity in the cytoplasm and
163 nucleus at 100%. In the absence of FLAG-V2, we found 43% of V1-YFP was
164 associated with the nuclear fraction but decreased to 11% in the presence of
165 FLAG-V2. We concluded from these results that V2 is able to change the nuclear
166 localization of V1 protein.
167

168 **V2 Protein Interacts with V1 Protein**

169 We set out to understand the underlying mechanism by which V2 protein affects
170 the subcellular localization of V1 protein by first testing whether there is an
171 interaction between V2 and V1 proteins by using a co-immunoprecipitation (Co-IP)
172 assay. FLAG-tagged V2 (FLAG-V2) was co-expressed with YFP or V1-YFP in *N.*
173 *benthamiana*. Total protein extracts were subject to immunoprecipitation by using
174 FLAG-trap beads, and the resulting precipitates were analyzed using an anti-YFP
175 antibody or an anti-FLAG antibody. Although a similar amount of FLAG-V2 was
176 pulled down with FLAG-trap beads, only V1-YFP, but not YFP, was detected (Fig
177 2a), even though both YFP and V1-YFP were well expressed (Fig 2a).

178 The fact that V1 protein was co-precipitated with V2 protein suggests that V2
179 protein may bind to V1 to form a V1-V2 protein complex. To confirm the V1-V2
180 interaction and identify the location where the V1 and V2 proteins may form a
181 complex, we used a bimolecular fluorescence complementation (BiFC) assay. A
182 positive interaction between nYFP-V1 and cYFP-V2 was observed in both the
183 cytoplasm and perinuclear region, as indicated by the presence of reconstituted green
184 fluorescence (Fig 2b). We also noticed a faint fluorescence signal inside the nucleus.
185 It should be noted that V1-YFP also localized in the cytoplasm and the perinuclear
186 region when it was co-infiltrated with FLAG-V2 (Fig 1a), suggesting that V2 binds
187 V1 protein at the perinucleus and the cytoplasm. No green fluorescence signal was
188 generated when nYFP-V1 and cYFP, or nYFP and cYFP-V2, or nYFP and cYFP

189 were co-expressed (Fig 2b), reinforcing a specific interaction between V2 and V1
190 proteins in plant cells.
191
192 **V2 Mediates the Nucleocytoplasmic Shuttling of V1 Protein Through Host**
193 **Exportin-α**
194 V2 can change the nuclear localization of the V1 protein, decreasing its
195 accumulation in the nucleus. These results raised the possibility that V2 might help
196 V1 protein export from the nucleus to the cytoplasm. Because the nuclear export of
197 proteins is often mediated by exportin-α, we tested the subcellular localization of V2
198 upon treatment with leptomycin B (LMB), an inhibitor of exportin-α [33]. As
199 expected, the level of nuclear-localized V2-YFP was increased after LMB treatment
200 in epidermal cells of H2B-RFP transgenic *N. benthamiana* plants (Fig 3a), suggesting
201 that V2 depends on exportin-α to move out of the nucleus. To confirm our
202 observations, we performed a nuclear-cytoplasmic fractionation assay on H2B-RFP
203 transgenic *N. benthamiana* plants expressing V2-YFP with or without LMB treatment.
204 H2B-RFP and PEPC were used as nuclear- and cytoplasmic-localized marker proteins,
205 respectively. About 32% of the total V2-YFP accumulated in the nucleus and
206 increased to 54% with the LMB treatment (Fig 3b), agreeing well with our imaging
207 results (Fig 3a).
208 We also checked whether V2-mediated V1-YFP nuclear export can be affected
209 by the LMB treatment. Co-expressed with FLAG-V2, V1-YFP had very low

accumulation in the nucleus (Fig 1a), but a strong nuclear signal was observed after treatment with LMB (top panel, -DMSO, Fig 3c), suggesting that V2-mediated V1 protein nucleocytoplasmic shuttling is similar to the V2 protein export, which depends on exportin-α.

To confirm the specific effect of LMB on localizations of the V1 and V2 proteins, we further infiltrated LMB-treated cells with 0.5% dimethyl sulfoxide (DMSO), which degrades LMB. As expected, the V1-YFP signal was detected in the nucleus in the presence of FLAG-V2 and LMB at the beginning of DMSO treatment (top panel, -DMSO, Fig 3c). However, the V1-YFP signal in the nucleus decreased gradually after a longer DMSO treatment that eliminated the inhibitory effect of LMB (Fig 3c).

To verify the nucleocytoplasmic shuttling of the V1-V2 complex, we performed a BiFC assay applying the same treatments as above. In the presence of LMB only, the reconstituted YFP signal was strongly detected in the nucleus (Fig 3d), indicating that the V1-V2 complex was also present in the nucleus as well as in the cytoplasm and perinuclear region (Fig 2b). After DMSO treatment for 2 hours, the nucleus-localized YFP signal clearly diminished, indicating an exportin-α-mediated nucleocytoplasmic shuttling of the V1-V2 complex (Fig 3d). These results indicated that the nucleocytoplasmic shuttling of V1 protein is dependent on the V1-V2 interaction and exportin-α.

The V2 Mutants C85A Abolishes the V1-V2 Interaction

231 To verify that the V1-V2 interaction plays a crucial role in the V1 nuclear export
232 and to identify the approximate sites in V2 that are responsible for the interaction, we
233 constructed six V2 mutants, each with single or double substitutions (Fig 4a). We then
234 tested their interactions with V1 protein using the Co-IP assay. Among the six V2
235 mutants, only the $V2^{C85A}$ mutant, which has a cysteine to alanine substitution in the
236 residue at position 85, was not pulled down along with FLAG-V1 (Fig 4a,4b).
237 Alanine substitution did not affect expression and stability of the $V2^{C85A}$ mutant
238 because V2-YFP and $V2^{C85A}$-YFP accumulated at similar levels (top Input panel, Fig
239 4b).
240 It is well-known that V2 protein is involved in PTGS by binding to tomato SGS3
241 (SlSGS3), a homologue of Arabidopsis SGS3 protein [34]. It has been confirmed that
242 a mutant of V2 ($V2^{C84A/C86A}$) does not interact with SlSGS3 and lost its function as a
243 suppressor of gene silencing [34]. Given the fact that C85 is adjacent to C84 and C86,
244 it is possible that $V2^{C85A}$ may be dysfunctional not only in interacting with V1 protein
245 but also with SlSGS3. To this end, we confirmed that $V2^{C85A}$, but not $V2^{C84AC86A}$,
246 interacted with SlSGS3 in the yeast two-hybrid system (Fig 4c), indicating that the
247 C85A substitution specifically blocked the V1-V2 interaction but did not disrupt other
248 functions of the V2 protein, such as the ability to interact with SlSGS3 that leads to a
249 block of host gene silencing-mediated host defense. To further confirm that C85,
250 rather than C84 and C86, is required for different V2 roles, we also tested the ability
251 of $V2^{C84A/C86A}$ (Fig 4a) to interact with V1 protein. The Co-IP assay indicated that the

252 $V2^{C84A/C86A}$ mutant interacted with the V1 protein (Fig 4d). Taken together, the
253 activities of the V2 protein in interacting with V1 protein and SlSGS3 can be
254 separated, where the C85A mutation blocks V2 protein's interaction with V1 protein
255 but not with SlSGS3.
256
257 **The $V2^{C85A}$ Mutant Fails to Redistribute the V1 Protein**
258 After confirming that $V2^{C85A}$ accumulated well and interacted with SlSGS3, we
259 next checked the localization of $V2^{C85A}$ by expressing YFP-tagged $V2^{C85A}$
260 ($V2^{C85A}$-YFP) in *N. benthamiana*. The fluorescence signal was observed in the
261 cytoplasm and perinuclear region (Fig 5a), similar to wild-type (wt) V2-YFP, in 56%
262 of cells expressing $V2^{C85A}$-YFP (Fig 5b). In 44% of cells, however, the fluorescence
263 signal was more spread than that of V2-YFP and was localized in an elongated region
264 that does not exactly surround the DAPI-stained nucleus (Fig 5a). The nature of the
265 localization remains to be determined. The C85A mutation did not affect the
266 expression and stability of V2-YFP as $V2^{C85A}$-YFP accumulated at a similar level as
267 V2-YFP (Fig 5c). These results indicated that C85 has some effects on the perinuclear
268 localization and the nuclear export function of the V2 protein.
269 To test the effect of $V2^{C85A}$ on the localization of V1, FLAG- $V2^{C85A}$ was
270 co-expressed with V1-YFP in *N. benthamiana* cells. A strong V1-YFP signal was
271 detected in the nucleus in the presence of FLAG- $V2^{C85A}$, similar to that when
272 V1-YFP was expressed alone (Fig 5d). Among 50 cells that were observed for the

localization of V1 protein, no obvious difference in the V1-YFP distribution pattern was observed in the absence or presence of $V2^{C85A}$ (Fig 5e), suggesting that $V2^{C85A}$ was not able to affect the nuclear localization of V1 protein. Because V1 protein accumulated at similar levels in the absence or presence of $V2^{C85A}$ (Fig 5f), we propose that the disrupted V1-V2 interaction is responsible for the failed redistribution of V1-YFP in the presence of $V2^{C85A}$.

A C85 Substitution in V2 Protein Delays Viral Systemic Infection

To assess the role of the V1-V2 interaction in viral infection, we constructed an infectious TYLCV clone with a substitution in the C85 of V2 coding sequence. As V2 ORF overlaps with V1 ORF in the TYLCV genome, mutations in V2 may affect V1 amino acid sequence. To ensure that changes in C85 has no effect on V1 protein in TYLCV genome, the C85S mutation was introduced into a TYLCV clone to generate TYLCV-C85S, based on the fact that V2-C85S mutant did not interact with V1 protein (S1a Fig), but interacted with SlSGS3 (S1b Fig), and did not affect the subcellular localization of V1-YFP (S1c Fig). TYLCV-C85S and TYLCV were used to inoculate *solanum lycopersicum* and *N. benthamiana* plants.

Fifteen tomato plants were inoculated with either wt TYLCV or TYLCV-C85S. Typical symptoms such as chlorosis on leaves were first observed at 16 days post agro-infection (dpai) on tomato plants inoculated with TYLCV. No obvious symptoms were observed in the plants inoculated with TYLCV-C85S at 16 dpai (Fig

294 6a). The vast majority of TYLCV-C85S-inoculated tomato plants remained
295 symptomless even at 32 dpai and only 1-2 plants among 15 eventually developed mild
296 symptoms eventually, such as leaf yellowing (Fig 6b). Real-time PCR showed that
297 viral DNA accumulation was much lower in plants inoculated with TYLCV-C85S
298 than in plants inoculated with wt TYLCV (Fig 6c). Almost no virus particles
299 accumulated in the TYLCV-C85S-inoculated plants based on a Western blotting
300 assay using an anti-CP antiserum at 16 dpai (Fig 6d).

301 Similar results were also obtained in TYLCV-C85-inoculated *N. benthamiana*
302 plants. All wt TYLCV-inoculated plants showed typical symptoms at 22 dpai, such as
303 leaf yellowing and curling, but only one out of fifteen plants inoculated with
304 TYLCV-C85S showed mild symptoms (Fig 7a, 7b). Accumulated TYLCV genomic
305 DNA (Fig 7c) and virus particles (Fig 7d) in systemic leaves of
306 TYLCV-C85S-inoculated plants were much lower than those in wt
307 TYLCV-inoculated plants.

308 These results collectively showed that the mutation at C85 of V2 protein caused
309 significant low levels of virus accumulation in the systemic leaves and dramatic
310 decrease of the infection efficiency with delayed and mild symptoms.

311

312 ## Discussion

313 Because genome replication of geminiviruses takes place in the nucleus of the
314 infected host cells [5], it is crucial to transport the viral offspring DNAs from the

315 nucleus back to the cytoplasm for intracellular, cell-to-cell, and long-distance
316 movement. In bipartite geminiviruses, it is well-known that BV1 protein encoded by
317 the DNA-B component facilitates trafficking of the viral genome into and out of the
318 host nucleus [6-9, 35]. However, monopartite geminiviruses, which do not contain the
319 DNA-B component, does not encode BV1 protein. So, the viral DNA shuttling
320 between the nucleus and the cytoplasm is accomplished by protein or a protein
321 complex encoded by the DNA-A component. It has been reported that V1 protein of
322 monopartite geminiviruses mediates the import and export of viral DNA [13, 17, 28].
323 However, V1 protein might not be the only viral protein that is involved in the
324 nucleocytoplasmic shuttling of TYLCV. Previous reports based on triple
325 microinjection experiments revealed that the nuclear export of DNA was enhanced
326 20–30% in the presence of V2 (V2+V1+viral DNA), suggesting that V2 enhances
327 nuclear export of viral DNA [13]. But the mechanism by which V2 protein promotes
328 viral DNA export is unclear. We report here that V2 may facilitate viral DNA export
329 by interacting with V1 and promoting the nuclear export of V1 protein.
330 In this study, we found that V2 protein localized primarily in the perinuclear
331 region and the cytoplasm (Fig 1b). A very weak signal was also present in the nucleus
332 (Fig 1b, 1c), but upon treatment with the exportin-α inhibitor LMB, the amount of
333 nucleus-localized V2 protein increased significantly (Fig 3a), suggesting V2 protein
334 shuttles between the nucleus and the cytoplasm but is quickly exported out of the
335 nucleus via exportin-α. It is unclear, however, how V2 imported into the nucleus.

Our work indicates that V2 plays a critical role in the nuclear export of V1 protein as the nucleus-localized V1 diminished when V2 was present (Fig 1a). Supporting this notion, we found that LMB treatment, which prevented V2 from exporting out of the nucleus (Fig 3a), blocked V2-mediated nuclear export of V1 (Fig 3c). We also showed that the specific V1-V2 interaction is closely related to V1 trafficking. The V1-V2 interaction primarily occurred at the perinuclear region and the cytoplasm (Fig 2b) but was strongly detected in the nucleus upon LMB treatment (Fig 3d), suggesting that they may be in a complex or complexes throughout the viral replication and movement in infected cells. In addition, it also suggested that LMB only specifically blocked V2's transport out of the nucleus but had no effect on the V1-V2 interaction. However, our data are not able to determine whether V2 mediates the nuclear import of V1 protein. In addition, our results do not rule out the possibility that other viral proteins, such as C4 protein, may also be involved in this process.

Cysteine at 85 of V2 was found to be crucial for the V1-V2 interaction because substitutions of Cys85 with alanine (Fig 4b) or serine (S1a Fig) led to substantially inhibited interaction with V1 and thus, its ability to facilitate V1's transport out of the nucleus (Fig 5d, 5e for C85A and S1c Fig for C85S). Because V1 is known for binding to and facilitating nucleocytoplasmic trafficking of viral DNA [13, 17, 28], and because V2 facilitates the nuclear export of viral DNA along with V1 [13], we propose that the V2-promoted nuclear export of viral DNA is via the V1-V2 interaction. Our hypothesis is consistent with our results that the TYLCV-C85S

357 mutant, which has the C85S mutation incorporated into an infectious TYLCV clone,
358 led to the delayed onset of symptoms with only mild symptoms only in 1-2 tomato or
359 *N. benthamiana* plants out of a total of 15 (Fig 6a, 6b, 7a, 7b). Real-time PCR and
360 Western blotting assay results confirmed significant reduction in viral accumulation in
361 TYLCV-C85S-inoculated plants compared with those plants inoculated by wt
362 TYLCV (Fig 6c, 6d, 7c, 7d). These results showed that the cysteine at 85 of V2 was
363 very important for viral systemic infection. The mutant on C85 caused V2 to lose its
364 ability to bind with V1 and lead to V2 being unable to help with V1 accumulation at
365 the perinuclear region nor participate in V1-mediated nuclear export of viral genomic
366 DNA, which eventually affected the viral systemic infection.

367 In monopartite geminiviruses, V2 is a multifunctional protein that is involved in
368 suppressing host PTGS and TGS, pathogenicity and systemic infection [5,30,31,32].
369 Substitution in cysteine 85 may affect functions other than its interaction with V1,
370 especially since both Cys84 and Cys86 are critical for interacting with SlSGS3 and
371 the suppression of gene silencing [34]. We found that even though the C85A (Fig 4b)
372 and C85S (S1a Fig) mutants failed to interact with V1 protein and thus, V1's
373 trafficking out of the nucleus (Fig 5d, 5e, S1c), but both interacted with SlSGS3 (Fig
374 4c, S1b), suggesting that C85A and C85S mutants maintain their activity as gene
375 silencing suppressors. These results also are consistent with the notion that the C85S
376 mutation delays viral systemic infection by affecting V1-mediated viral genomic
377 DNA transportation from the nucleus to the cytoplasm, not by disturbing gene

silencing-mediated host defense. However, we cannot totally rule out the possibility that other V2-mediated viral infection step(s) besides viral DNA trafficking are affected by the C85S mutation.

Our data also showed that the C84A/C86A double mutant interacted with V1 (Fig 4d) but not SlSGS3 (Fig 4c), indicating that C84 and C86 are not related to V2's ability to interact with V1. Our results therefore revealed that motifs responsible for V1's nuclear export and gene silencing suppressor activity are independent from one another.

Our results indicate that V2 binds to V1 protein and facilitate the nuclear export of V1. During TYLCV infection, V1 mediates both nuclear import and export of viral DNA. The equilibrium between nuclear targeting and nuclear egress is changed upon completion of replication and the V1-V2 interaction can improve the nuclear export of the V1-DNA complex. Thus, viral DNA will be preferentially transported out of the nucleus for subsequent infection events. In the presence of the $V2^{C85S}$ mutant, the nuclear export of V1 is slowed down or eliminated and therefore, viral DNA and subsequent viral cell-to-cell and systemic movement is delayed. However, we cannot totally rule out that the V1-V2 complex is also required for intracellular, cell-to-cell, and/or long-distance movement besides nuclear export of V1 protein and V1-mediated viral offspring DNAs.

Based on our findings here, we propose a working model for the role of V2 in V1-mediated nuclear export of TYLCV genomic DNA (Fig 8). When offspring viral

399 genomic DNA are produced in the nucleus, they are bound by V1 [29]. A V2-V1-viral
400 DNA complex is subsequently formed via a specific interaction between V1 and V2
401 and, with the help of exportin-α, V2 facilitates the V1-viral DNA complexes to egress
402 from the nucleus to the perinucleus and the cytoplasm with an enhanced efficiency.
403 Eventually TYLCV then spreads to adjacent cells and upper leaves, which results in a
404 systemic infection. The infection efficiency and the accumulation of TYLCV in the
405 systemic leaves are dramatically decreased without a defective V2-V1 interaction.
406 In summary, our results revealed that one mechanism of V2 protein's
407 involvement in viral DNA transportation is to promote V1-mediated viral
408 transportation from the nucleus to the perinuclear region and the cytoplasm, which is
409 with a specific interaction with V1, form V2-V1-viral DNA complex, and via host
410 exportin-α. However, whether V2 promotes the ability of V1 to bind viral DNA and
411 whether the V1-V2 interaction works after nuclear transportation require further
412 research.
413

414 # Materials and Methods

415 ## Plant Materials and Growth Conditions

416 Transgenic *Nicotiana benthamiana* plants expressing a nuclear marker,
417 H2B-RFP (red fluorescent protein fused to the C terminus of histone 2B) [36], were
418 kindly provided by Dr. Xiaorong Tao (Nanjing Agricultural University, Nanjing,
419 China).

All agro-infiltration experiments were performed in wild-type (wt) or H2B-RFP transgenic *N. benthamiana*. Plants were grown in a growth chamber (ModelGXZ500D, Jiangnan Motor Factory, Ningbo, China) at 26°C (16 h, light) and 22°C (8 h, dark) for 4-6 weeks before being infiltrated with the agrobacterium. After infiltration, the plants were kept under the same growth conditions.

Plasmid Construction

The coding sequences of TYLCV V2 and V1 genes were amplified from the cDNA of a TYLCV-infected tomato plant from Jiangsu Province, China (GenBank accession number GU111505) [37], using corresponding primers (S1 Table). Site-specific mutants of $V2^{G70A}$, $V2^{S71A}$, $V2^{K73A}$, $V2^{C85A}$, $V2^{C84AC86A}$, $V2^{C85S}$, $V2^{T96A}$ were synthesized (Invitrogen, China) and confirmed by sequencing (Fig 4a).

To investigate the subcellular localization, the TYLCV V2 (*Bgl*II), V1 genes (*Bam*HI) and $V2^{C85A}$, $V2^{C84AC86A}$, $V2^{C85S}$ were amplified using specific primers (Supplementary Table S1). Yellow fluorescent protein (YFP) tag was inserted between the CaMV 35S promoter and the 35S terminator (35St) in the pCambia1300 binary vector to construct the p1300-YFP vector as previously described [38]. Then, amplified products were individually inserted either into the *Bam*HI or *Bgl*II (compatible with *Bam*HI) site of the p1300-YFP vector to fuse in frame with YFP at the N-terminus or C-terminus to generate V2-YFP, V1-YFP, YFP-V2 and $V2^{C85A}$-YFP, $V2^{C84AC86A}$-YFP, $V2^{C85S}$-YFP.

To make BiFC vectors, full-length coding sequences of V2 and V1 genes were amplified using the primers listed in Supplemental Table S1, then V1 was cloned into the *Bam*HI site as a fusion with the N-terminal fragment of YFP and V2 was cloned into the *Bam*HI site as a fusion with the C-terminal fragment of YFP, resulting in nYFP-V1 and cYFP-V2.

FLAG tagged V2 and V1 were amplified by PCR using specific primers (S1 Table) and inserted into the *Bam*HI site between the 35S promoter and the 35St in the pCambia1300 binary vector to generate FLAG-V2 and FLAG-V1 for the further Co-IP experiments.

For the yeast two-hybrid assay, V2, $V2^{C85A}$, $V2^{C84AC86A}$, $V2^{C85S}$ were amplified and inserted into the *Nde*I/*Eco*RI-digested pGADT7 vector and SlSGS3 was cloned into the *Nde*I/*Bam*HI-digested pGBDT7 vector.

Agro-infiltration Assays in *N. benthamiana*

Target vectors were transformed into *A. tumefaciens* strain GV3101 by electroporation. Agrobacterial cultures were harvested when the OD600 was approximately 0.8–1.0, collected by centrifugation, resuspended in the induction buffer (10 mM MgSO4, 100 mM 2-N-morpholino ethanesulfonic acid [pH 5.7], 2 mM acetosyringone), and incubated for 2 h at room temperature. The suspensions were then adjusted to OD600=0.5 and infiltrated into 4- to 6-week-old wt *N. benthamiana* or H2B-RFP transgenic *N. benthamiana* leaves for the further experiments.

461 **Subcellular Localization of Proteins**

462 P1300-YFP, YFP-V2, V2-YFP, V1-YFP, V2 ^{C84AC86A} and V2^{C85A}-YFP were
463 individually introduced into *A. tumefaciens* strain GV3101 through electroporation.
464 Leaves of 4-week-old *N. benthamiana* plants were infiltrated with *A. tumefaciens*
465 harbouring the designated constructs. At 40 hours post infiltration (hpi), plants leaves
466 were excised and YFP fluorescence was examined in epidermal cells using confocal
467 microscopy (Zeiss LSM 880). The microscope was configured with a 458–515 nm
468 dichroic mirror for dual excitation and a 488-nm beam splitter to help separate YFP
469 fluorescence.

470 **Bimolecular Fluorescence Complementation (BiFC) Assay**

471 BiFC experiments were performed as previously described [39] with minor
472 modifications. nYFP-V1 and cYFP-V2 were introduced individually into *A.*
473 *tumefaciens* strain GV3101 by electroporation. After overnight growth and activation,
474 agrobacterium cultures were combined and infiltrated into leaves of *N. benthamiana*
475 as above. After agroinfiltration, *N. benthamiana* plants were grown in a growth
476 chamber with a 16 h light/8 h dark cycle. YFP fluorescence was observed and
477 photographed by using confocal microscopy (Zeiss LSM 710) at 48 hpi. YFP was
478 observed under a mercury lamp light using a 488-nm excitation filter. Photographic
479 images were prepared using ZEN 2011SP1.

480 **Co-Immunoprecipitation**

481 The Co-IP assay was performed as previously described [38]. 40 h after
482 infiltration, *N. benthamiana* leaves were harvested and ground in liquid nitrogen.
483 Proteins were extracted in IP buffer (40 mM Tris-HCl at pH 7.5, 100 mM NaCl, 5
484 mM MgCl2, 2 mM EDTA, 2×EDTA-free proteinase inhibitor, 1 mM PMSF, 4 mM
485 DTT, 1% glycerol, and 0.5% Triton-X100). After centrifugation, the supernatant was
486 mixed with FLAG-conjugated beads (Sigma, USA). After 1 h incubation at 4°C, the
487 beads were washed six times with IP buffer, resuspended in 2×SDS gel loading buffer,
488 and boiled for 10 min. The samples were loaded onto a 12% (vol/vol) SDS/PAGE gel
489 and target proteins were detected using a polyclonal anti-GFP antibody (GenScript,
490 USA) or a monoclonal anti-FLAG (Sigma, USA) antibody.

491 **Yeast Two-Hybrid Assay**

492 The yeast two-hybrid system was used to examine interactions between V2,
493 $V2^{C85A}$, $V2^{C84AC86A}$ and SlSGS3. V2, $V2^{C85A}$, and $V2^{C84AC86A}$ were cloned into the
494 activation domain (AD)-containing vector and SlSGS3 was cloned into the vector
495 harboring the DNA binding domain (BD). Both constructs were transformed into
496 *Saccharomyces cerevisiae* strain AH109. The plasmid pairs BD-53 and AD-recT
497 served as a positive controls, while the plasmid pairs BD-Lam and AD-recT were
498 used as a negative controls. Transformants were grown at 30°C for 72 h on
499 SD/-His/-Leu/-Trp/ synthetic medium to test for protein-protein interaction.

500 **Nuclear-Cytoplasmic Fractionation Assay**

Nuclear-cytoplasmic fractionation assays were performed as described previously [40] with minor modifications. Infiltrated leaves were harvested and mixed with 2 mL/g of lysis buffer (20 mM Tris-HCl, pH 7.5, 20 mM KCl, 2 mM EDTA, 2.5 mM MgCl2, 25% glycerol, 250 mM Sucrose, 5 mM DTT and 10 mM protease inhibitor). The homogenate was filtered through a double layer of Miracloth. The supernatant, consisting of the cytoplasmic fraction, was centrifuged at 10,000 rpm for 10 min at 4°C and collected. The pellet was resuspended with 500 µL of NRB2 (20 mM Tris-HCl, pH 7.5, 0.25 M Sucrose, 10 mM MgCl2, 0.5% Triton X-100, 5 mM b-mercaptoethanol and 10 mM protease inhibitor) and overlaid on top of 500 µL NRB3 (20 mM Tris-HCl, pH 7.5, 1.7 M Sucrose, 10 mM MgCl2, 0.5% Triton X-100, 5 mM b-mercaptoethanol and 10 mM protease inhibitor). These were centrifuged at 12,000 rpm for 40 min at 4°C. The final nuclear pellet was resuspended in 400 µL lysis buffer. As quality controls for the fractionation assays, PEPC protein and H2B-RFP were used as a cytoplasmic and a nuclear marker, respectively.

Leptomycin B Treatment Assays

Leptomycin B (LMB) Treatment Assays were performed as previously described [19] with minor modifications. LMB (Fisher Scientific, USA) was dissolved in ethanol to prepare 10 mM stock solutions. For *in vivo* treatment of *N. benthamiana* leaves, stock solutions were diluted in water to prepare solutions of 10 nM LMB. Agroinfiltrated *N. benthamiana* leaves expressing the protein of interest at 40 hpi were infiltrated with 10 nM LMB. 2 h after LMB treatment, the leaves were cut and

mounted on a glass slide for confocal imaging. When needed, DMSO was further infiltrated into LMB-treated leaves and tissues were harvested at the specified time points, namely 1, 1.5, and 2 h.

TYLCV constructs for Agrobacterium-mediated inoculation

For the construction of infectious clones of TYLCV containing $V2^{C85S}$, a full length TYLCV mutant, TYLCV-C85S (the cysteine residue on V2 at amino acid 85 was changed to serine), was synthesized (Invitrogen, China). Then the full DNA-A of TYLCV-C85S was amplified using the primers listed in S1 Table and inserted into the pGEM-T Easy (Promega, USA) vector to produce pGEM-1A-C85S. After sequence confirmation, a 2183 nucleotide (nt) fragment was excised from pGEM-1A with *Bam*HI and *Sac*I, then subcloned into the *Bam*HI-*Sac*I sites of the binary vector pBinPLUS to produce pBinPLUS-0.8A. The full-length of TYLCV-C85S was digested from pGEMT-1A with *Bam*HI and inserted into pBinPLUS-0.8A at its unique *Bam*HI site to get pBinPLUS-1.8A, the infectious clone of TYLCV-C85S. The wt TYLCV infectious clone was constructed as previously described [38].

Agrobacterium cultures harboring TYLCV constructs were injected into the stem of *S. lycopersicum* and *N. benthamiana* with a syringe. Inoculated plants were grown in an insect-free cabinet with supplementary lighting corresponding to a 16-h day length.

RNA extraction and qRT-PCR analysis

542 Total RNA was extracted from mock (Agrobacterium-carrying empty vector)-,
543 wt TYLCV- or TYLCV-C85S-infiltrated *S. lycopersicum* or *N. benthamiana* leaves at
544 different time periods using the Trizol Reagents (Life technologies, USA) and treated
545 with DNase I following the manufacturer's instructions (PrimeScript RT reagent Kit
546 with gDNA Erase, Takara, Japan). cDNA synthesized from reverse transcription of
547 RNA samples was used to determine the mRNA expression levels of target genes as
548 well as for quantifying TYLCV accumulation levels at the date indicated. *SlActin* or
549 *NbActin* was used as an internal control for tomato or *N. benthamiana*, respectively.
550

551 ## Acknowledgements

552 We thank Dr. Sue Tolin (Virginia Tech, USA) and Dr. Janet Webster (Virginia
553 Tech, USA) for critical reading of the manuscript. We are grateful to Xiaorong Tao
554 (Nanjing Agricultural University, China) for kindly providing the H2B-RFP
555 transgenic *N. benthamiana*.
556

557 ## References

558 1. Gafni Y. Tomato yellow leaf curl virus, the intracellular dynamics of a plant DNA virus.
559 *Mol. Plant Pathol.* 2003; 4: 9-15.
560 2. Moriones E, Navas-Castillo J. Tomato yellow leaf curl virus, an emerging virus complex
561 causing epidemics worldwide. *Virus Res.* 2000; 71: 123-134.
562 3. Nakhla MK, Maxwell DP. Epidemiology and management of tomato yellow leaf curl

563 disease. *Plant Virus Dis. Control* 1997; 43: 565-583.

564 4. Glick E, Levy Y, Gafni Y. The viral etiology of Tomato yellow leaf curl disease-a review.
565 *Plant Prot. Sci.* 2009; 45: 81-97.

566 5. Hanley-Bowdoin L, Bejarano ER, Robertson D, Mansoor S. Geminiviruses: masters at
567 redirecting and reprogramming plant processes. *Nat. Rev. Microbiol.* 2013; 11: 777-788.

568 6. Brough CL, Hayes RJ, Morgan AJ, Coutts RHA, Buck KW. Effects of mutagenesis in
569 vitro on the ability of cloned tomato golden mosaic virus DNA to infect *Nicotiana*
570 *benthamiana* plants. *J. Gen. Virol.* 1988; 69: 503-514.

571 7. Etessami P, Callis R, Ellwood S, Stanley J. Delimitation of essential genes of cassava
572 latent virus DNA 2. *Nucleic Acids Res.* 1988; 16: 4811-4829.

573 8. Jeffrey JL, Pooma W, Petty ITD. Genetic requirements for local and systemic movement
574 of tomato golden mosaic virus in infected plants. *Virology* 1996; 223: 208-218.

575 9. Sudarshana MR, Wang HL, Lucas WJ, Gilbertson RL. Dynamics of bean dwarf mosaic
576 geminivirus cell-to-cell and long-distance movement in *Phaseolus vulgaris* revealed,
577 using the green fluorescent protein. *Mol. Plant Microbe Interact.* 1998; 11: 277-291.

578 10. Padidam M, Beachy RN, Fauquet CM. Tomato leaf curl geminivirus from India has a
579 bipartite genome and coat protein is not essential for infectivity. *J. Gen. Virol.* 1995; 76:
580 25-35.

581 11. Lazarowitz SG, Beachy RN. Viral movement proteins as probes for intracellular and
582 intercellular trafficking in plants. *Plant Cell* 1999; 11: 535-548.

583 12. Liu H, Boulton MI, Oparka KJ, Davies JW. Interaction of the movement and coat proteins

of Maize streak virus: implications for the transport of viral DNA. *J. general virology* 2001; 82(1): 35-44.

13. Rojas MR, Jiang H, Salati R, Xoconostle-Cazares B, Sudarshana MR, Lucas WJ, et al. Functional analysis of proteins involved in movement of the monopartite begomovirus, Tomato yellow leaf curl virus. *Virology* 2001; 291(1): 110-125.
14. Gafni Y, Epel BL. The role of host and viral proteins in intra- and inter-cellular trafficking of geminiviruses. *Mol. Plant Pathol.* 2002; 60(5): 231-241.
15. Boulton MI, Pallaghy CK, Chatani M, MacFarlane S, Davies JW. Replication of Maize streak virus mutants in maize protoplasts: evidence for a movement protein. *Virology* 1993; 192(1): 85-93.
16. Boulton MI, Steinkellner J, Donson J, Markham PG, King DI, Davies JW. Mutational analysis of virion-sense genes of maize streak virus. *J. Gen. Virol.* 1989; 70: 2309-2323.
17. Kunik T, Mizrachy L, Citovsky V, Gafni Y. Characterization of a tomato karyopherin that interacts with the Tomato yellow leaf curl virus (TYLCV) capsid protein. *J. Exp*. Bot. 1999; 50: 731-732.
18. Yaakov N, Levy Y, Belausov E, Gaba V, Lapidot M, Gafni Y. Effect of a single amino acid substitution in the NLS domain of Tomato yellow leaf curl virus-Israel (TYLCV-IL) capsid protein (CP) on its activity and on the virus life cycle. *Virus Res.* 2011; 158(1-2): 8-11.
19. Mei Y, Wang Y, Hu T, Yang X, Lozano-Duran R, Sunter G, et al. Nucleocytoplasmic shuttling of geminivirus C4 protein Mediated by phosphorylation and myristoylation is

605 critical for viral pathogenicity. *Mol. plant* 2018; 11(12): 1466-1481.

606 20. Rojas MR, Hagen C, Lucas WJ, Gilbertson RL. Exploiting chinks in the plant's armor:
607 evolution and emergence of Geminiviruses. *Annu. Rev. Phytopathol.* 2005; 43(1):
608 361-394.

609 21. Navot N, Pichersky E, Zeidan M, Zamir D, Czosnek H. Tomato yellow leaf curl virus: A
610 whitefly-transmitted geminivirus with a single genomic component. *Virology* 1991; 185:
611 151-161.

612 22. Diazpendon JA, Canizares MC, Moriones E, Bejarano ER, Czosnek H, Navas-castillo J.
613 Tomato yellow leaf curl viruses: ménage a trois between the virus complex, the plant and
614 the whitefly vector. *Mol. Plant Pathol.* 2010; 11(4): 441-450.

615 23. Scholthof KBG, Scott A, Henryk C, Palukaitis P, Jacquot E, Hohn T, et al. Top 10 plant
616 viruses in molecular plant pathology. *Mol. Plant Pathol.* 2011; 12(9): 938-944.

617 24. Zrachya A, Glick E, Levy Y, Arazi T, Citovsky V, Gafni Y. Suppressor of RNA silencing
618 encoded by Tomato yellow leaf curl virus-Israel. *Virology* 2007; 358(1): 159-165.

619 25. Wang B, Li F, Huang C, Yang X, Qian Y, Xie Y, et al. V2 of tomato yellow leaf curl virus
620 can suppress methylation-mediated transcriptional gene silencing in plants. *J. Gen. Virol.*
621 2014; 95(1): 225-230.

622 26. Barziv A, Levy Y, Hak H, Mett A, Belausov E, Citovsky V, et al. The (TYLCV) V2
623 protein interacts with the host papain-like cysteine protease CYP1. *Plant Signal. Behav.*
624 2012; 7(8): 983-989.

625 27. Wartig L, Kheyr PA, Noris E, Kouchkovsky FD, Jouanneau F, Gronenborn B, et al.

626 Genetic analysis of the monopartite tomato yellow leaf curl geminivirus: roles of V1, V2,
627 and C2 ORFs in viral pathogenesis. *Virology* 1997; 228(2): 132-140.
628 28. Kunik T, Palanichelvam K, Czosnek H, Citovsky V, Gafni Y. Nuclear import of the capsid
629 protein of Tomato yellow leaf curl virus (TYLCV) in plant cells. *Plant J.* 1998;13:
630 393-399.
631 29. Palanichelvam K, Kunik T, Citovsky V, Gafni Y. The capsid protein of tomato yellow leaf
632 curl virus binds cooperatively to single-stranded DNA. *J. Gen. Virol.* 1998; 79 (11):
633 2829-2833.
634 30. Fondong VN. Geminivirus protein structure and function. *Mol. Plant Pathol.* 2013; 14:
635 635-649.
636 31. Jeske H. Geminiviruses. *Curr. Top. Microbiol. Immunol.* 2009; 331: 185-226.
637 32. Sahu PP, Sharma N, Puranik S, Muthamilarasan M, Prasad M. Involvement of host
638 regulatory pathways during geminivirus infection: a novel platform for generating durable
639 resistance. *Funct. Integr. Genomics* 2014; 14: 47-58.
640 33. Mathew C, Ghildyal R. CRM1 inhibitors for antiviral therapy. *Frontiers in*
641 *microbiology* 2017; 8: 1171.
642 34. Glick E, Levy Y, Gafni Y. The viral etiology of Tomato yellow leaf curl disease-a review.
643 *Plant Prot. Sci.* 2009; 45: 81-97.
644 35. Ye J, Yang J, Sun Y, Zhao P, Gao S, Jung C, et al. Geminivirus activates ASYMMETRIC
645 LEAVES 2 to accelerate cytoplasmic DCP2-mediated mRNA turnover and weakens RNA
646 silencing in *Arabidopsis*. *PLoS Pathog.* 2015; 11(10): e1005196.

647 36. Martin K, Kopperud K, Chakrabarty R, Banerjee R, Brooks R, Goodin MM. Transient
648 expression in *Nicotiana benthamiana* fluorescent marker lines provides enhanced
649 definition of protein localization, movement and interactions in planta. *Plant J.* 2009; 59:
650 150–162.
651 37. Ji Y, Xiong R, Cheng Z, Zhou T, Zhao T, Yu W, et al. Molecular diagnosis of Tomato
652 yellow leaf curl disease in Jiangsu province. *Acta Hortic*. 2008; 35(12): 1815-1818.
653 38. Zhao W, Ji Y, Wu S, Ma X, Li S, Sun F, et al. Single amino acid in V2 encoded by
654 TYLCV is responsible for its self-interaction, aggregates and pathogenicity. *Sci. Rep.*
655 2018, 8(1).
656 39. Shen Q, Liu Z, Song F, Xie Q, Hanley-Bowdoin L, Zhou X. Tomato SlSnRK1 protein
657 interacts with and phosphorylates βC1, a pathogenesis protein encoded by a geminivirus
658 β-satellite. *Plant Physiol.* 2012; 157(7): 1394-406.
659 40. Wang W, Ye R, Xin Y, Fang X, Li C, Shi H, et al. An importin ß protein negatively
660 regulates microRNA activity in *Arabidopsis*. *Plant Cell* 2011; 23(10): 3565-3576.

661

662 # Additional Information

663

664 ## Funding

665 This study was financially supported by grants from the National Key R&D
666 Program of China (No. 2018YFD0201208), Jiangsu Agriculture Science and
667 Technology Innovation Fund [No. CX(18)2005], China Agriculture Research System

668 (No. CARS-24-C-01), National Natural Science Foundation of China (No. 31572074,
669 31770168) and Jiangsu Academy of Agricultural Sciences Fund (No. 6111614).

670

671 **Author contributions**

672 Y.Z., Y.J., X.W. and W.Z. designed the project. W.Z., S.W. and E.B. conducted
673 experiments. All authors analyzed the data and reviewed the manuscript. W.Z., Y.J.
674 and X.W. wrote the paper.

675

676 **Competing financial interests**

677 The authors declare no competing financial interests.

678

679 ## Supporting Information

680

681 **S1 Table Primers used in this study**

	Designation	Sequence(5' to 3')	Assay
1	V1-bF	CGGGATCCATGTCGAAGCGACCAGGCG A	V1-YFP, nYFP-V1
2	V1-bR	CGGGATCCATTTGATATTGAATCATAG AAATAG	V1-YFP, nYFP-V1, FLAG-V1
3	FLAG-V1-F	CGGGATCCATGGATTACAAGGATGATG	FLAG-V1

		ATGATAAGTCGAAGCGACCAGGCGA	
4	V2-bgF	GAAGATCTATGTGGGATCCACTTCTAA AT	V2-YFP, cYFP-V2, $V2^{C85A}$-YFP
5	V2-bgR	GAAGATCTGGGCTTCGATACATTCTGTA T	V2-YFP, cYFP-V2, $V2^{C85A}$-YFP, FLAG-V2, FLAG-$V2^{C85A}$
6	FLAG-V2-F	GAAGATCTATGGATTACAAGGATGATG ATGATAAGTGGGATCCACTTCTAAATG	FLAG-V2, FLAG-$V2^{C85A}$
7	TY-V2-F	CGCCATATGATGTGGGATCCACTTCTAA AT	AD-V2, AD-$V2^{C85A}$, AD-$V2^{C85S}$, AD-$V2^{C84AC86A}$
8	TY-V2-R	CGGAATTCTCAGGGCTTCGATACATTCT	AD-V2, AD-$V2^{C85A}$, AD-$V2^{C85S}$, AD-$V2^{C84AC86A}$
9	TY-1A-KF	GGGGTACCACTTCTAAATGAATTTCCTG	TYLCV-C85S

		AATCTG	
10	TY-1A-BR	CGGGATCCCACATAGTGCAAGACAAAC T	TYLCV-C85S
11	SlSGS3-F	CGCCATATGAGTTTCAGCAAATGGGGT GGG	BD-SlSGS3
12	SlSGS3-R	CGGGATCTCACATGGTGCCACTGCTATT GAC	BD-SlSGS3

682

683 **S1 Fig** (a) Co-IP assay showing that $V2^{C85S}$ does not interact with V1 protein. The
684 Co-IP assay was performed as in Fig 2a. (b) Analysis of the interaction between
685 SlSGS3 and wt V2 or the $V2^{C85S}$ mutant in the yeast two-hybrid assay. The Y2H
686 assay was performed as in Fig 4c. (c) Subcellular localization of V1 protein that was
687 co-expressed with FLAG-$V2^{C85S}$ in *N. benthamiana* cells. DAPI stains DNA in the
688 nucleus. Bars: 20 μm. Both V1-YFP and FLAG-$V2^{C85S}$ are expressed well as shown
689 by Western blot analysis.

690

691 ## Figures

692 **Fig 1** The effect of V2 protein on the nuclear distribution of V1 protein. (a) The
693 localization of V1 protein in the absence or presence of V2 protein in *N. benthamiana*
694 cells. V1-YFP was expressed in the absence or presence of FLAG-V2 and was
695 detected either by confocal microscopy (left panel) or by Western blotting using an

696 anti-GFP polyclonal antibody (right panel). DAPI stains DNA in the nucleus. Actin
697 serves as a control for equal loading of total lysates. Bars: 50 μm. (b) The localization
698 of V2 in *N. benthamiana* cells. The expressed YFP or YFP-V2 in epidermal cells of *N.*
699 *benthamiana* leaves was detected either by confocal microscopy (left panel) or by
700 Western blotting using an anti-GFP polyclonal antibody (right panel). DAPI stains
701 DNA in the nucleus. Bars: 50 μm. (c) Nuclear-cytoplasmic fractionation assay of the
702 distribution of V1 protein in the absence or presence of FLAG-V2 in H2B-RFP
703 transgenic *N. benthamiana* plants. Nuclei were purified from plant tissues expressing
704 V1-YFP in the absence or presence of FLAG-V2 using percoll density gradient
705 centrifugation. Western blot analysis was conducted with antibodies specific to the
706 indicated proteins using an anti-GFP polyclonal antibody or an anti-FLAG
707 monoclonal antibody. PEPC was used as a marker for the cytoplasmic fraction and
708 H2B-RFP was used as a marker for the nuclear fraction. Protein signal intensity was
709 measured by using Adobe Photoshop CS6, with the cytoplasm plus the nucleus levels
710 totaling as 100%.
711
712 **Fig 2** Identification of the interaction between V2 and V1 proteins. (a)
713 Co-immunoprecipitation (Co-IP) analysis of the interaction between FLAG-V2 and
714 V1-YFP. *N. benthamiana* leaves were co-infiltrated with *A. tumefaciens* cells
715 harbouring expression vectors to express FLAG-V2 and V1-YFP (Lane 1), FLAG-V2
716 and YFP (Lane 2), or V1-YFP alone (Lane 3). Cell lysates were incubated with

717 FLAG-trap beads (Sigma, USA). Samples before (Input) and after (IP)
718 immunoprecipitation were analyzed by immunoblotting using anti-GFP or -FLAG
719 antibody. (b) BiFC assays between V1 and V2 proteins in the leaves of *N.*
720 *benthamiana*. Confocal imaging was performed at 48 hpi. V1 and V2 were fused to
721 the N (nYFP) and C-terminal (cYFP) fragments of YFP, respectively. The V1-V2
722 interaction will lead to a reconstituted fluorescence signal. DAPI stains DNA in the
723 nucleus. Bars: 50 μm.
724
725 **Fig 3** The V2-mediated nuclear export of V1 protein is dependent on exportin-α. (a)
726 Subcellular distribution of V2-YFP without or with the LMB treatment in H2B-RFP
727 transgenic *N. benthamiana* plants. Leaf tissues were first agroinfiltrated with V2-YFP
728 for 40 hours and followed by 10 nM LMB for 2 hours. H2B-RFP signal represents the
729 nucleus. Bars: 50 μm. (b) Nuclear-cytoplasmic fractionation analysis of the
730 distribution of V2 with or without LMB treatment in H2B-RFP transgenic *N.*
731 *benthamiana* cells. Western blot analysis was conducted with antibodies specific to
732 the indicated proteins. PEPC was used as a marker for the cytoplasmic fraction and
733 H2B-RFP as a marker for the nuclear fraction. Protein signal intensity was measured
734 by using Adobe Photoshop CS6, the sum of cytoplasm plus the nucleus as 100%. (c)
735 Subcellular distribution of V1-YFP co-expressed with FLAG-V2 upon the treatment
736 of LMB and DMSO in H2B-RFP transgenic *N. benthamiana* plants. Leaf tissues
737 expressing V2-YFP and FLAG-V2 were first infiltrated with 10 nM LMB for 2 hours

738 followed by infiltration of 0.5% DMSO to degrade LMB. YFP signal was observed at
739 specific time points as indicated. Arrows indicate the V1-YFP signal in or around the
740 nucleus at different time points after the treatment with LMB and DMSO. H2B-RFP
741 signal represents the nucleus. Bars: 50 μm. (d) Effects of the LMB treatment on the
742 V1-V2 interaction as shown by BiFC in epidermal cells of H2B-RFP transgenic *N.*
743 *benthamiana* plants. Plant tissues co-expressing nYFP-V1 with cYFP-V2 were treated
744 with LMB for 2 h to inactivate exportin-α and then infiltrated with 0.5% DMSO to
745 degrade LMB. Confocal micrographs were taken at different time points after DMSO
746 treatment, as indicated. Arrow indicates localizations of the V1-V2 complex export
747 from the nucleus. Nuclei of *N. benthamiana* leaf epidermal cells are indicated by the
748 expression of the H2B-RFP transgene (red). Bars: 50 μm.
749
750 **Fig 4** Identification of the critical sites in V2 protein that are responsible for the
751 V1-V2 interaction. (a) Schematic illustration of the V2 protein. Nucleic acid and
752 amino acids sequences of V2 mutants, $V2^{G70A}$, $V2^{S71A}$, $V2^{K73A}$, $V2^{C85A}$, $V2^{C84AC86A}$,
753 and $V2^{T96A}$ are shown. (b) Co-IP assay to demonstrate the interaction between V1 and
754 wt V2 or $V2^{C85A}$. The Co-IP assay was performed as in Fig 2a. (c) Yeast-two hybrid
755 (Y2H) detecting possible interactions between SlSGS3 and $V2^{C85A}$ or $V2^{C84AC86A}$.
756 $V2^{C85A}$ and $V2^{C84AC86A}$ were fused with a GAL4 activation domain (AD-$V2^{C85A}$ and
757 AD-$V2^{C84AC86A}$), and SlSGS3 was fused to a GAL4-binding domain (BD-SlSGS3),
758 respectively. AH109 cells co-transformed with the indicated plasmids were subjected

759 to 10-fold serial dilutions and plated on synthetic defined medium SD/-His/-Leu/-Trp
760 medium to screen for positive interactions at 3 days after transformation. Yeast cells
761 co-transformed with AD-T+BD-53 serves as a positive control; yeast cells
762 co-transformed with AD-T+BD-Lam as a negative controls. (d) Co-IP assay to show
763 the interaction between V1 and V2 or $V2^{C84AC86A}$. The Co-IP assay was performed as
764 in Fig 2a.
765
766 **Fig 5** Characterization of the $V2^{C85A}$ mutant. (a) Subcellular localization of V2 and
767 $V2^{C85A}$. DAPI stains DNA in the nucleus. Bars: 50 μm. (b) Quantification of
768 perinuclear distribution of V2 and $V2^{C85A}$. The number of cells with perinuclear
769 distribution in different samples as in a. Experiments were repeated three times and 30
770 cells were observed in each trepeat. Values represent percentages of cells with a
771 perinuclear distribution of YFP signal ± SD (standard deviation). Data were analyzed
772 using Student's t-test and asterisks denote significant differences between V2-YFP-
773 and $V2^{C85A}$-YFP-infiltrated leaves (*$P < 0.05$). (c) Western blot analysis showing
774 accumulated V2 and $V2^{C85A}$ using anti-GFP polyclonal antibody. Actin serves as a
775 control for equal loading. (d) The localization of V1-YFP expressed alone or
776 co-expressed with $V2^{C85A}$ in *N. benthamiana* leaves. Bars: 20 μm. (e) Comparison of
777 the nucleus-localized V1-YFP in the absence or presence of $V2^{C85A}$. At least 150 cells
778 were analyzed from three independent repeats (at least 50 cells from each experiment.
779 Values represent mean ± SD relative to plants infiltrated with V1-YFP in the absence

780 or presence of $V2^{C85A}$. The data were analyzed using Student's t-test and no
781 significant difference was found for V1-YFP distribution between V1-YFP and
782 V1-YFP+ FLAG- $V2^{C85A}$. (f) The accumulated V1-YFP and FLAG- $V2^{C85A}$ as shown
783 by Western blot analysis.
784
785 **Fig 6** Effects of the C85S mutation on viral infection and viral accumulation in
786 TYLCV-inoculated tomato plants. (a) Symptoms in plants that were agro-inoculated
787 with wt TYLCV or TYLCV-C85S at 16 dpai. CK represents mock-inoculated plants.
788 Arrows point to the yellowing and curly leaves. (b) The infection time course of wt
789 TYLCV or TYLCV-C85S infection. Values represent percentages of systemically
790 infected plants at different DPAI and are given as mean ± SD of triplicate experiments.
791 In each experiment, 15 plants were inoculated and three independent repeats were
792 performed to confirm the results. (c) Viral DNA levels in plants as measured by
793 RT-PCR. Plants were inoculated with a wt TYLCV infectious clone or the
794 TYLCV-C85S, or mock-inoculated (CK). Accumulated levels of *V1 (CP)* were tested
795 at 3, 13, 23, and 33 dpai. Tomato leaves were agroinfiltrated with CK, TYLCV, or
796 TYLCV-C85S. Total RNAs were extracted from newly emerged leaves. Values
797 represent the mean relative to the CK-treated plants (n=3 biological replicates) and
798 were normalized with *SlActin* as an internal reference. (d) Western blot analyses of
799 accumulated V1 (CP), which represents viral particles, in CK, TYLCV and
800 TYLCV-C85S inoculated plants at 16 dpai.

Fig 7 Effects of the C85S mutation on viral infection and viral accumulation in TYLCV-inoculated *N. benthamiana*. (a) Symptoms in plants that were agro-inoculated with wt TYLCV or TYLCV-C85S at 16 dpai. CK represents mock-inoculated plants. Arrows point to the curly leaves. (b) The infection time course of wt TYLCV or TYLCV-C85S infection. Values represent percentages of systemically infected plants at different DPAI and are given as the mean ± SD of triplicate experiments. In each experiment, 15 plants were inoculated and three independent experiments were performed to confirm the results. (c) Viral DNA levels in plants inoculated with wt TYLCV infectious clone or TYLCV-C85S. Accumulated levels of *V1 (CP)* were tested at 3, 13, 23, and 33 dpai. *N. benthamiana* leaves were agroinfiltrated with CK, TYLCV, or TYLCV-C85S. Total RNAs was extracted from newly emerged leaves. Values represent the mean relative to the CK-treated plants (n=3 biological replicates) and were normalized with *NbActin* as an internal reference. (d) Western blot analyses of accumulated V1 (CP), which represents viral particles, in CK, TYLCV and TYLCV-C85S inoculated plants at 16 dpai.

Fig 8 A working model proposed for V2-mediated nucleocytoplasmic trafficking of V1 protein. Viral genomic DNAs are bound by V1 and import into the nucleus with the help of KAP α1 [17,18]. Via the specific interaction between V1 and V2, a

821 V2-V1-ssDNA complex is formed. With the help of exportin-α, V2 facilitates the

822 V1-ssDNA complexes to exit the nucleus to the perinucleus and the cytoplasm.

823

824 **Fig 1**

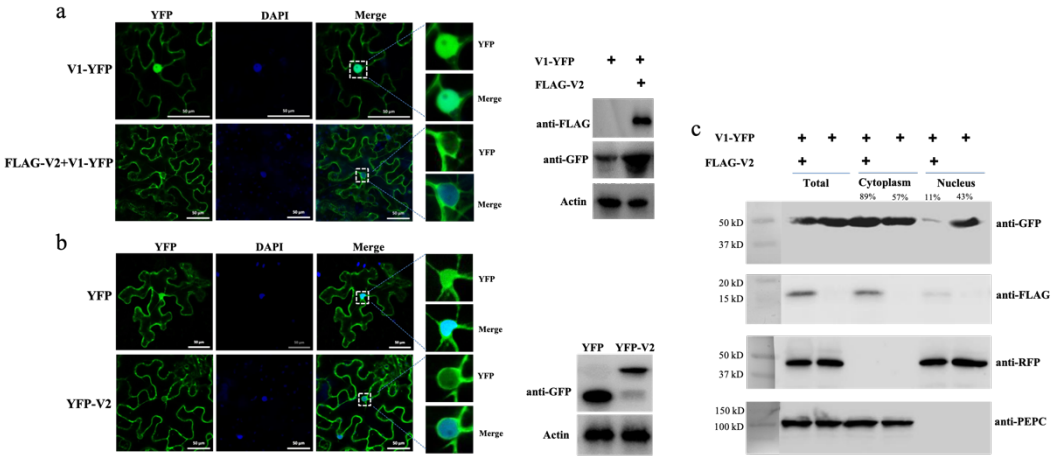

825

826

827 **Fig 2**

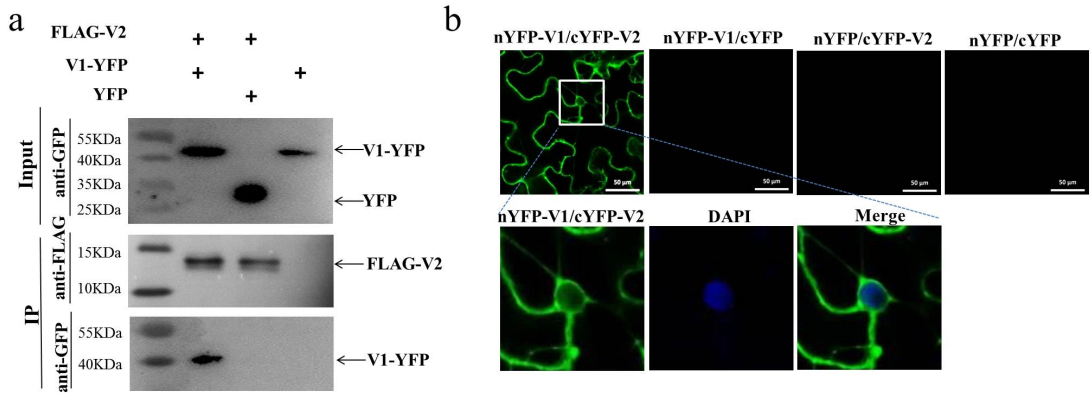

828

829

830

831

832

833 **Fig 3**

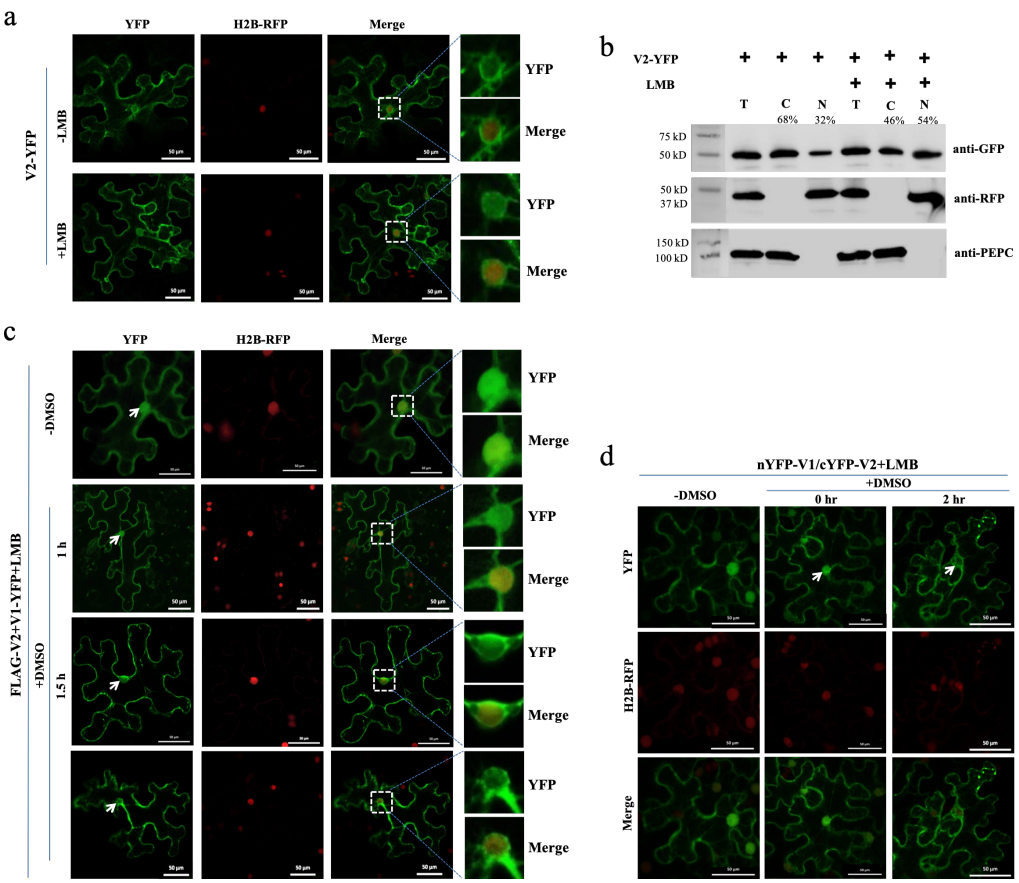

834

835 **Fig 4**

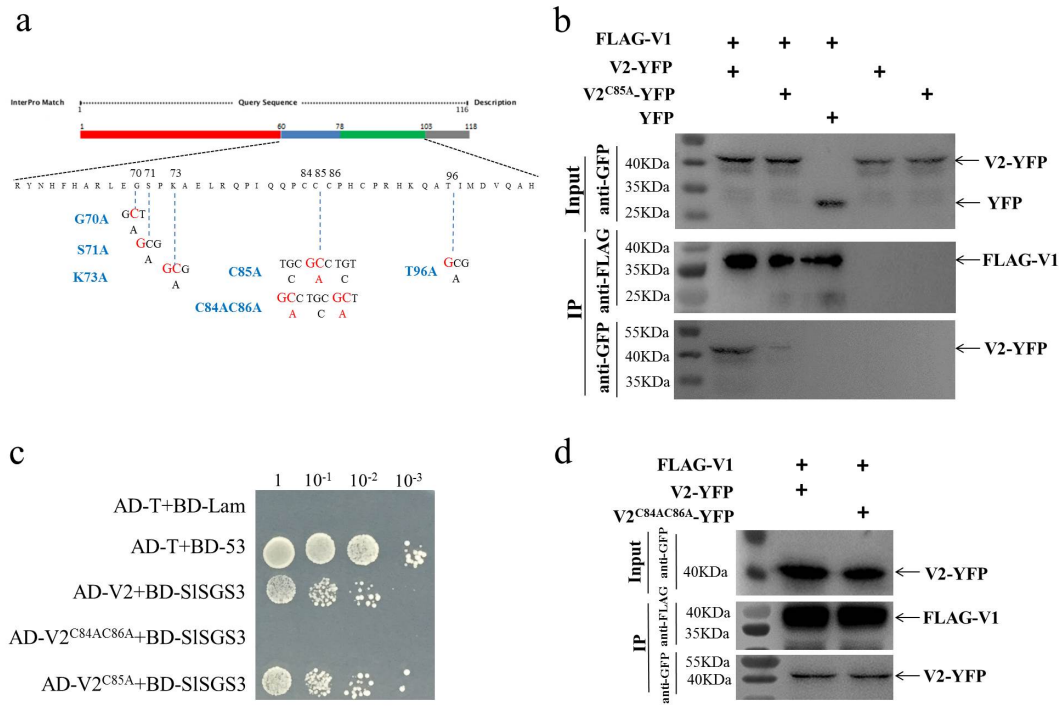

836

837 **Fig 5**

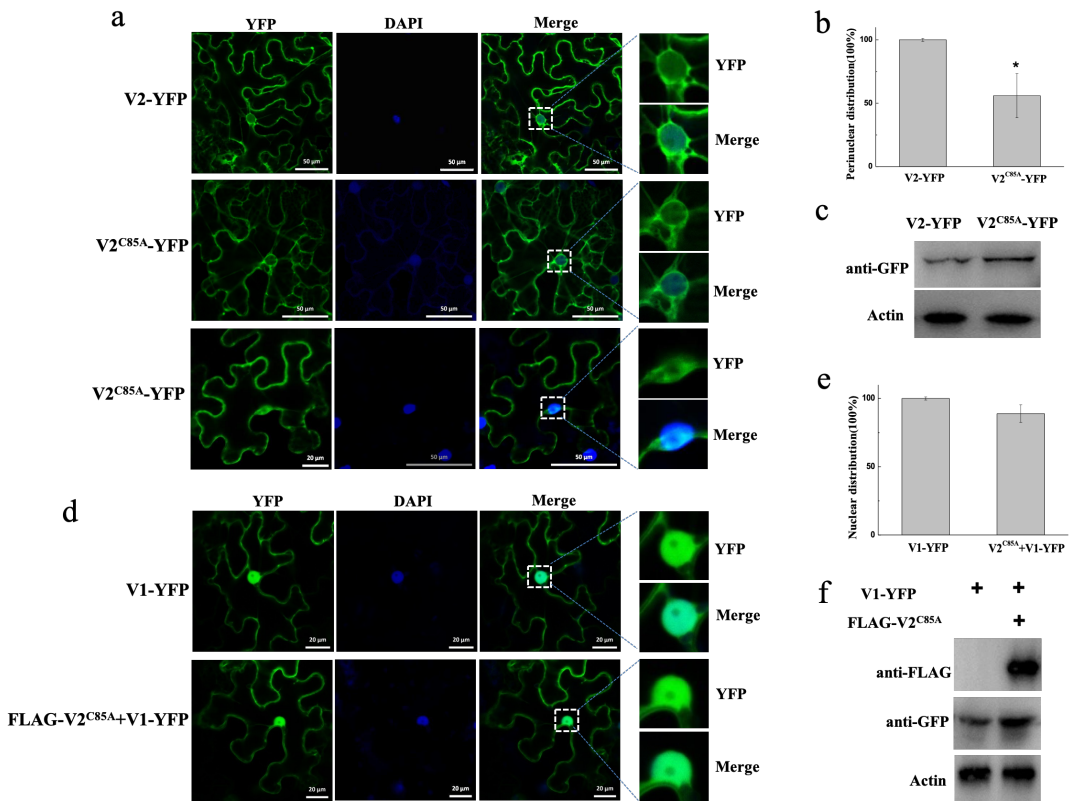

838

839 **Fig 6**

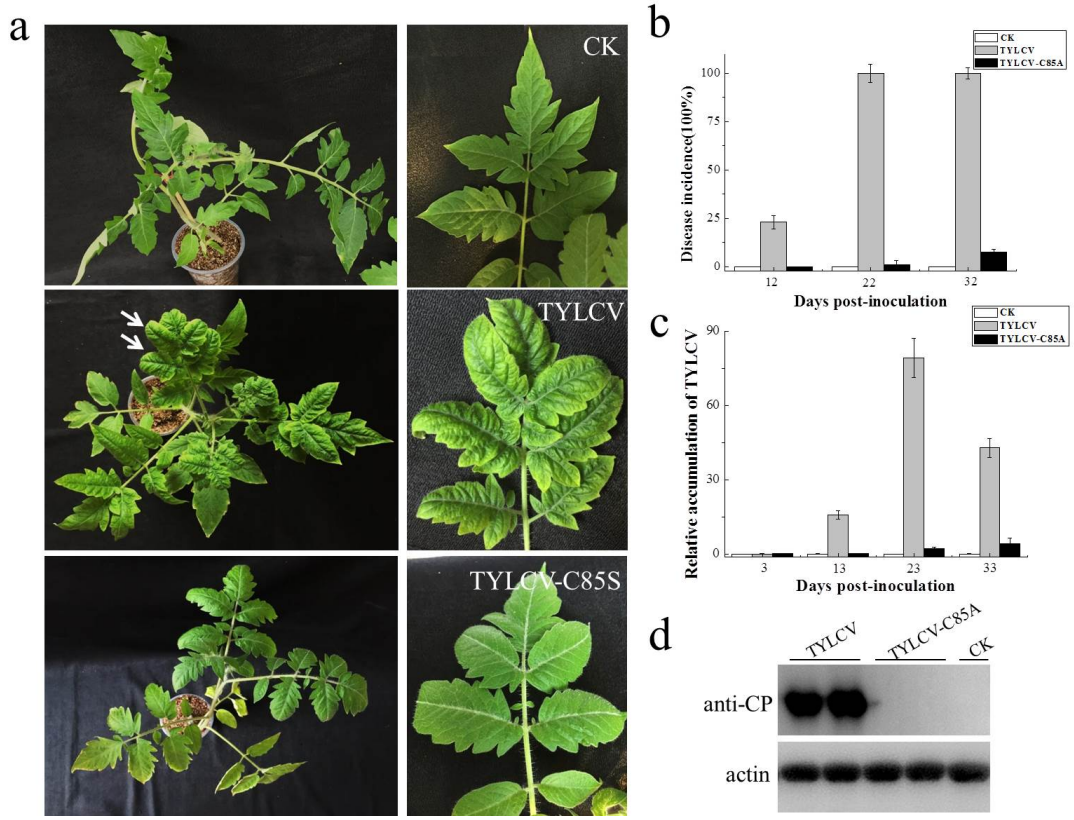

840

841 **Fig 7**

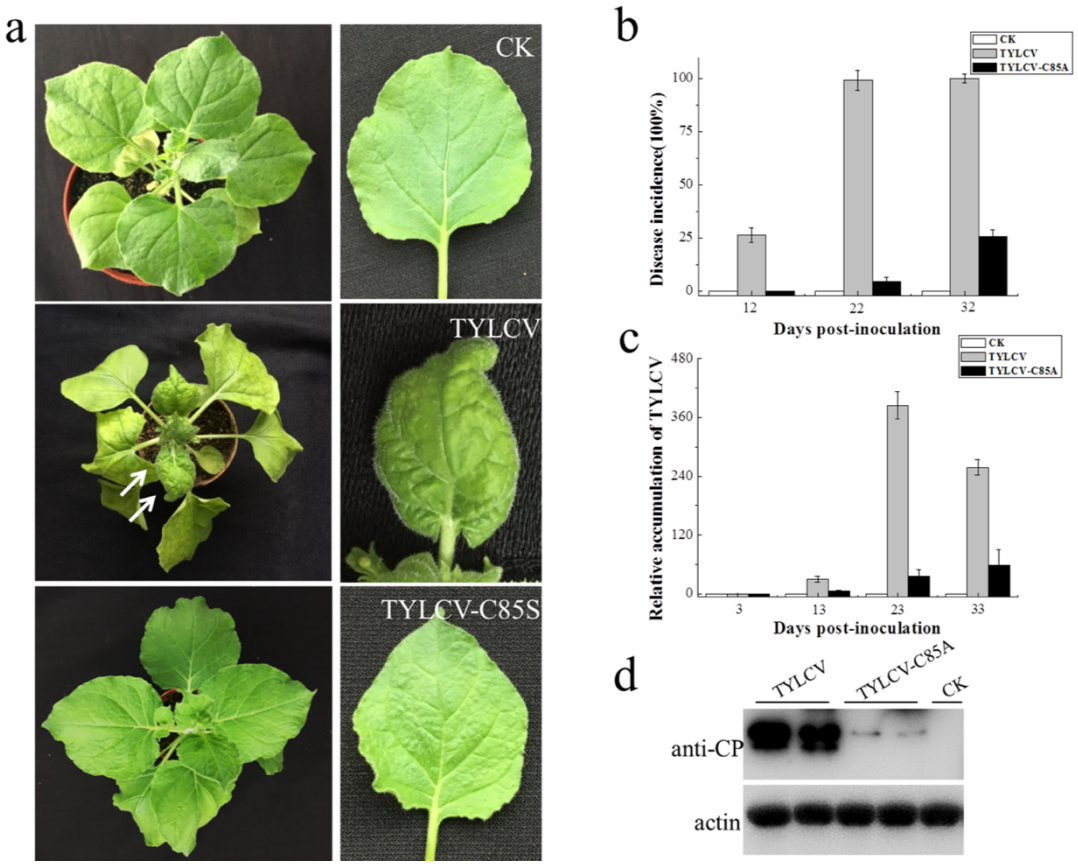

842

843

844 **Fig 8**

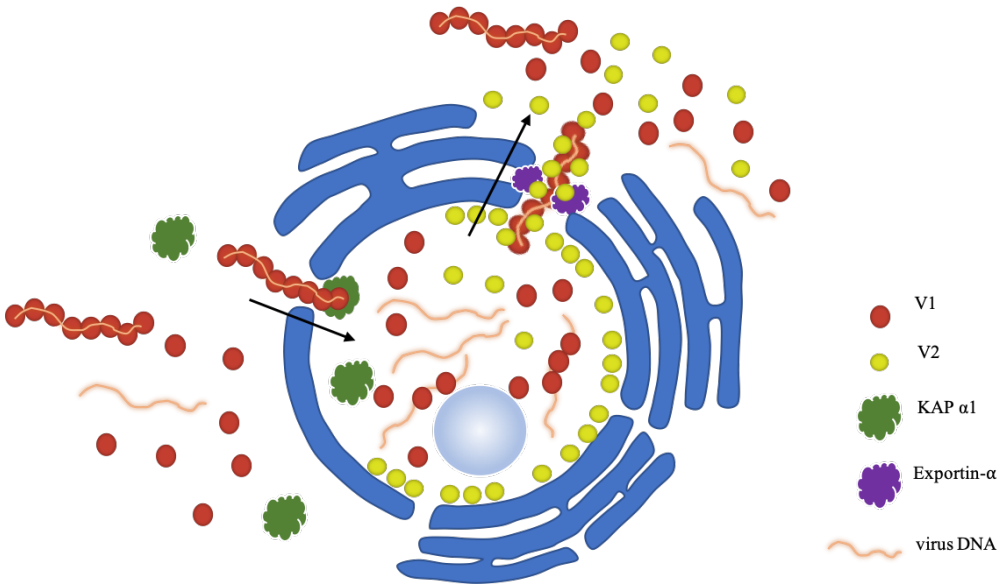

845

846

847 **S1 Fig**

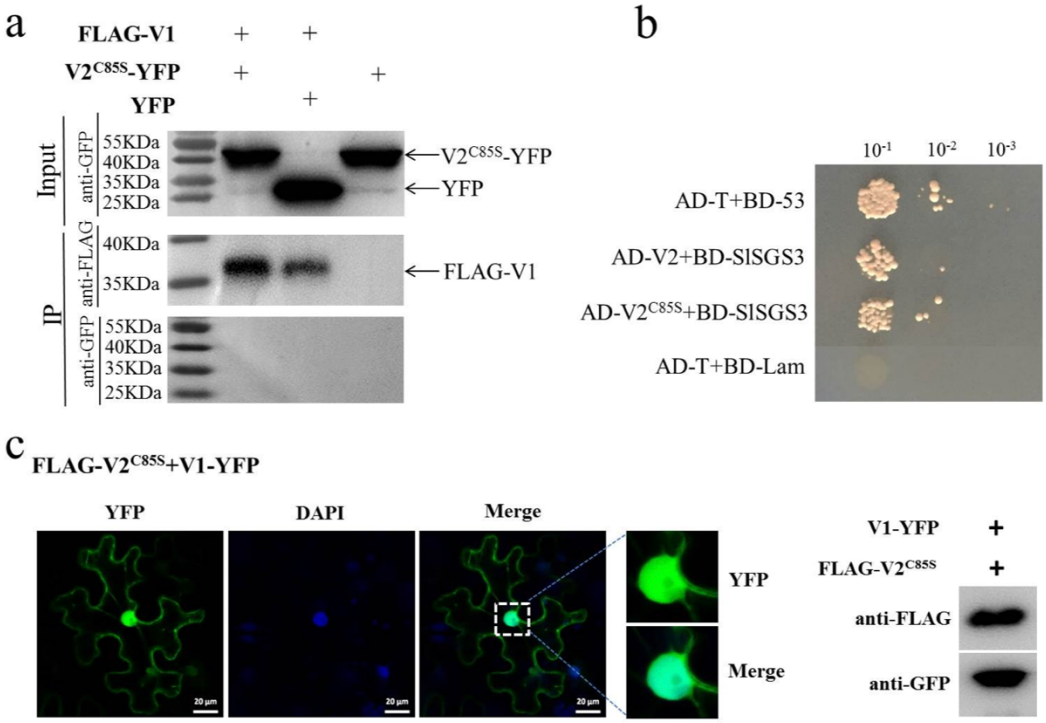

848

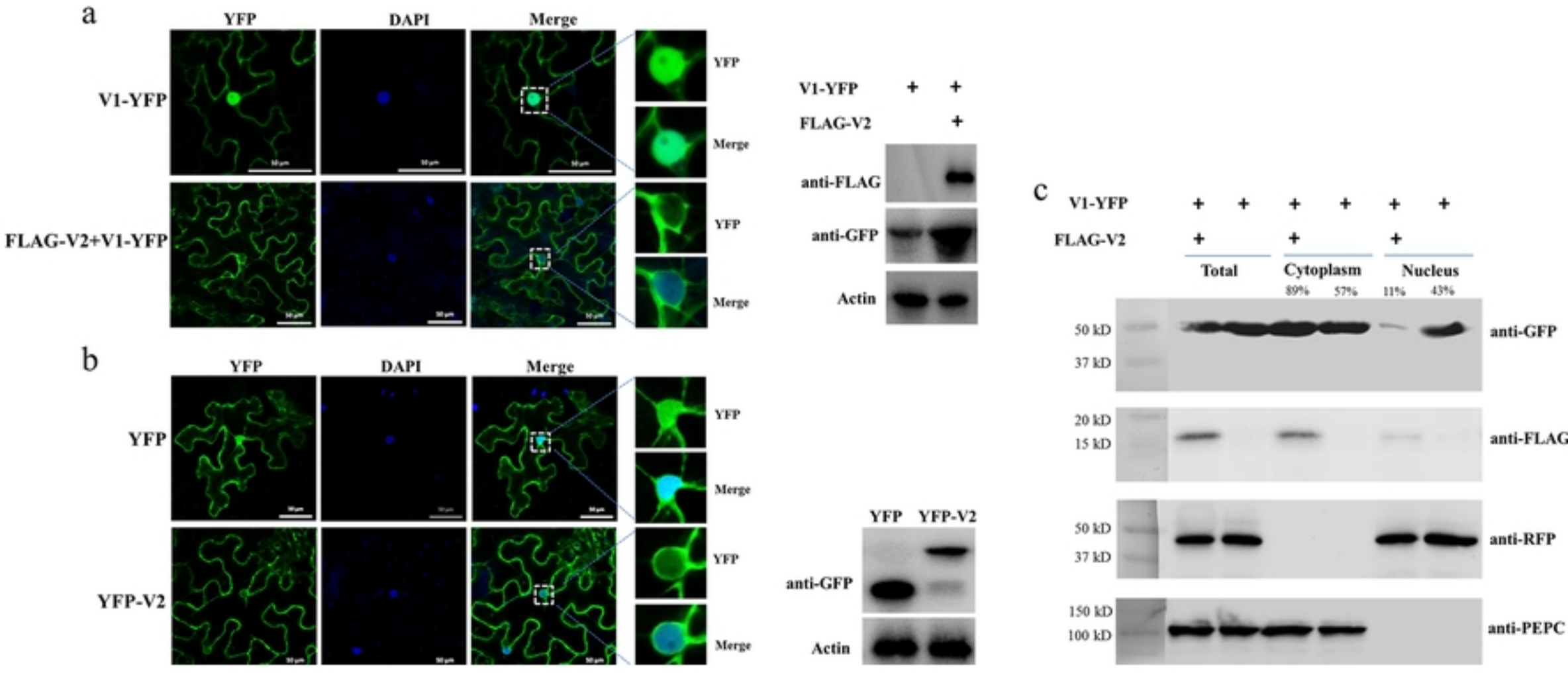
a
YFP
DAPI
Merge
V1-YFP
FLAG-V2+V1-YFP
YFP
Merge
YFP
Merge
V1-YFP + +
FLAG-V2 +
anti-FLAG
anti-GFP
Actin
b
YFP
DAPI
Merge
YFP
YFP-V2
YFP
Merge
YFP
Merge
YFP YFP-V2
anti-GFP
Actin
c
V1-YFP + + + + + +
FLAG-V2 + + +
Total
Cytoplasm
Nucleus
89% 57% 11% 43%
50 kD
37 kD
anti-GFP
20 kD
15 kD
anti-FLAG
50 kD
37 kD
anti-RFP
150 kD
100 kD
anti-PEPC

Fig 1

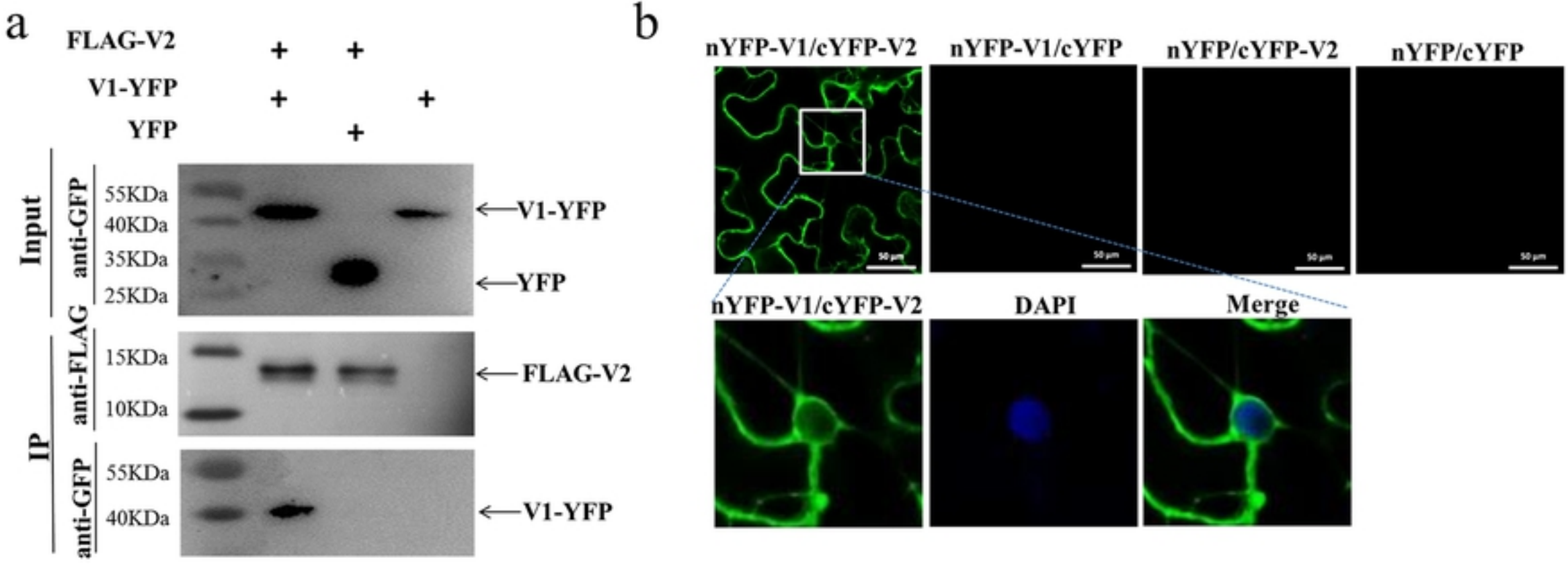
a
FLAG-V2
V1-YFP
YFP
+
+
+
+
Input
anti-GFP
55KDa
40KDa
35KDa
25KDa
←V1-YFP
←YFP
IP
anti-FLAG
15KDa
10KDa
←FLAG-V2
anti-GFP
55KDa
40KDa
←V1-YFP
b
nYFP-V1/cYFP-V2
nYFP-V1/cYFP
nYFP/cYFP-V2
nYFP/cYFP
nYFP-V1/cYFP-V2
DAPI
Merge

Fig 2

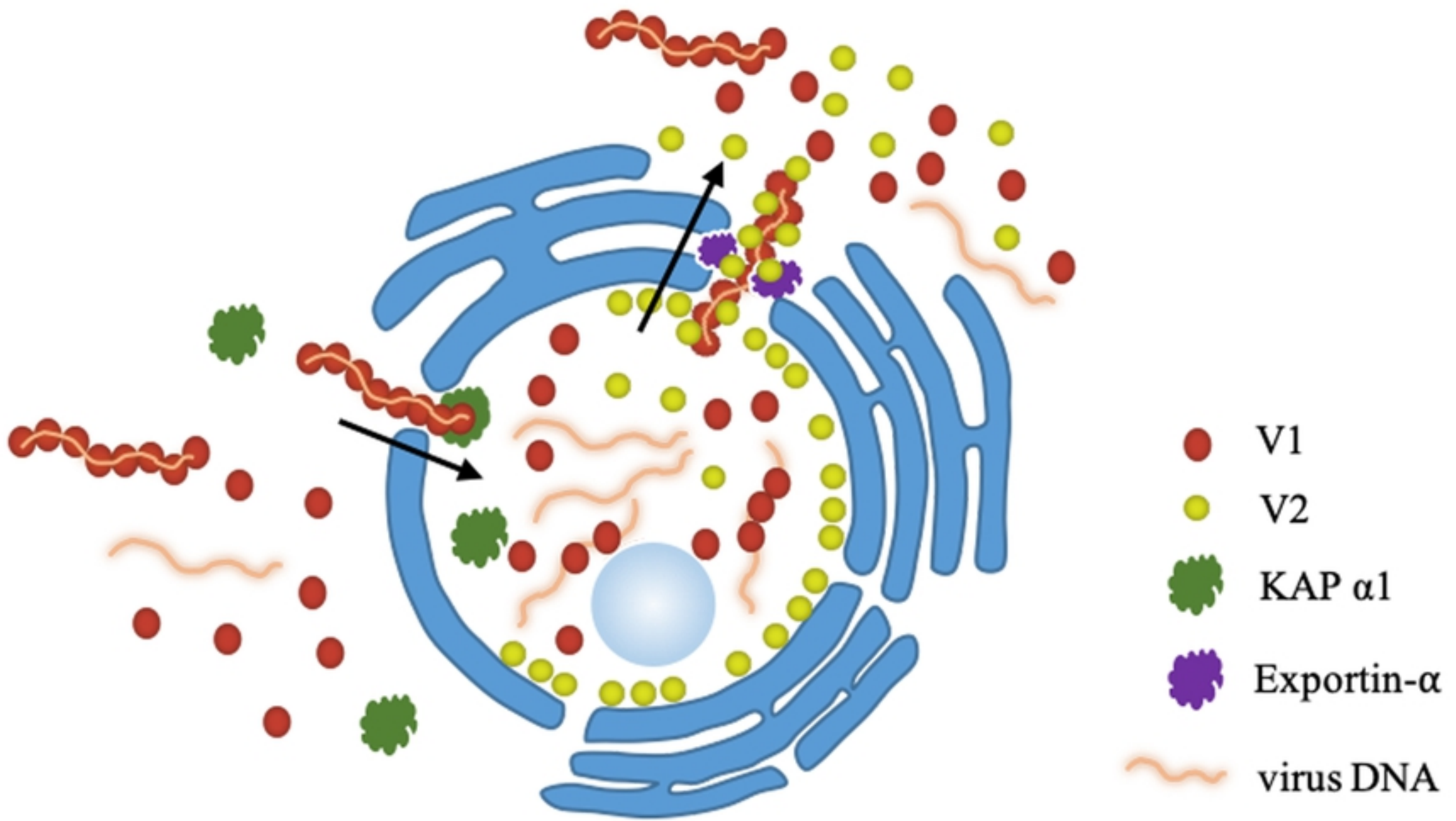

Fig 8

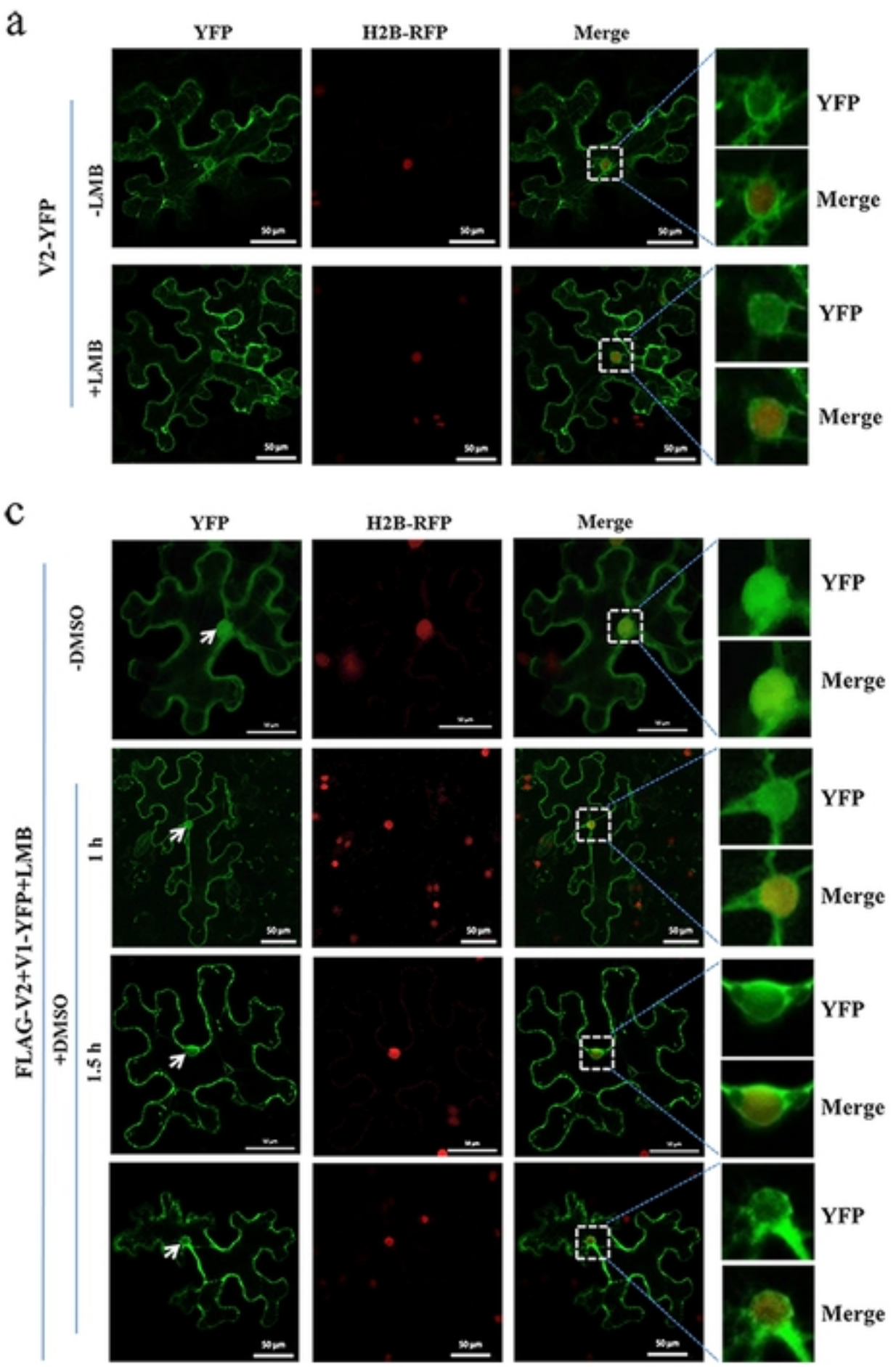
a
YFP
H2B-RFP
Merge
V2-YFP
-LMB
+LMB
YFP
Merge
b
V2-YFP
LMB
T
C
N
T
C
N
68%
32%
46%
54%
75 kD
50 kD
50 kD
37 kD
150 kD
100 kD
anti-GFP
anti-RFP
anti-PEPC
c
-DMSO
FLAG-V2+V1-YFP+LMB
+DMSO
1 h
1.5 h
d
nYFP-V1/cYFP-V2+LMB
-DMSO
+DMSO
0 hr
2 hr
YFP
H2B-RFP
Merge

Fig 3

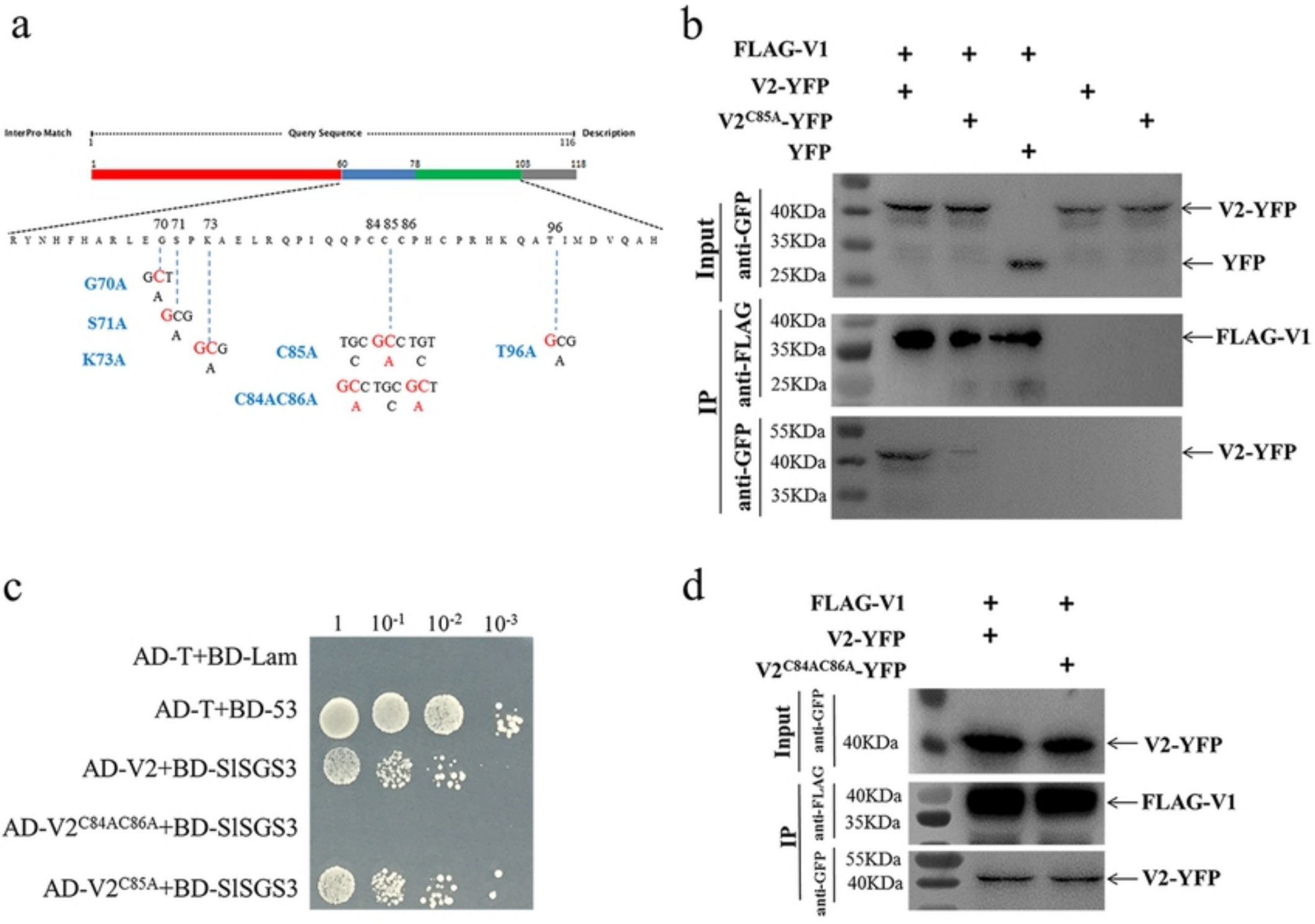
a
InterPro Match
Query Sequence
Description
1
116
1
60
78
103
118
70 71
73
84 85 86
96
R Y N H F H A R L E G S P K A E L R Q P I Q Q P C C C P H C P R H K Q A T I M D V Q A H
G70A
GCT
A
S71A
GCG
A
K73A
GCG
A
C85A
TGC GCC TGT
C A C
C84AC86A
GCC TGC GCT
A C A
T96A
GCG
A
b
FLAG-V1 + + +
V2-YFP + +
V2C85A-YFP + +
YFP +
Input
anti-GFP
40KDa
35KDa
25KDa
V2-YFP
YFP
IP
anti-FLAG
40KDa
35KDa
25KDa
FLAG-V1
anti-GFP
55KDa
40KDa
35KDa
V2-YFP
c
1 10-1 10-2 10-3
AD-T+BD-Lam
AD-T+BD-53
AD-V2+BD-SlSGS3
AD-V2C84AC86A+BD-SlSGS3
AD-V2C85A+BD-SlSGS3
d
FLAG-V1 + +
V2-YFP +
V2C84AC86A-YFP +
Input
anti-GFP
40KDa
V2-YFP
IP
anti-FLAG
40KDa
35KDa
FLAG-V1
anti-GFP
55KDa
40KDa
V2-YFP

Fig 4

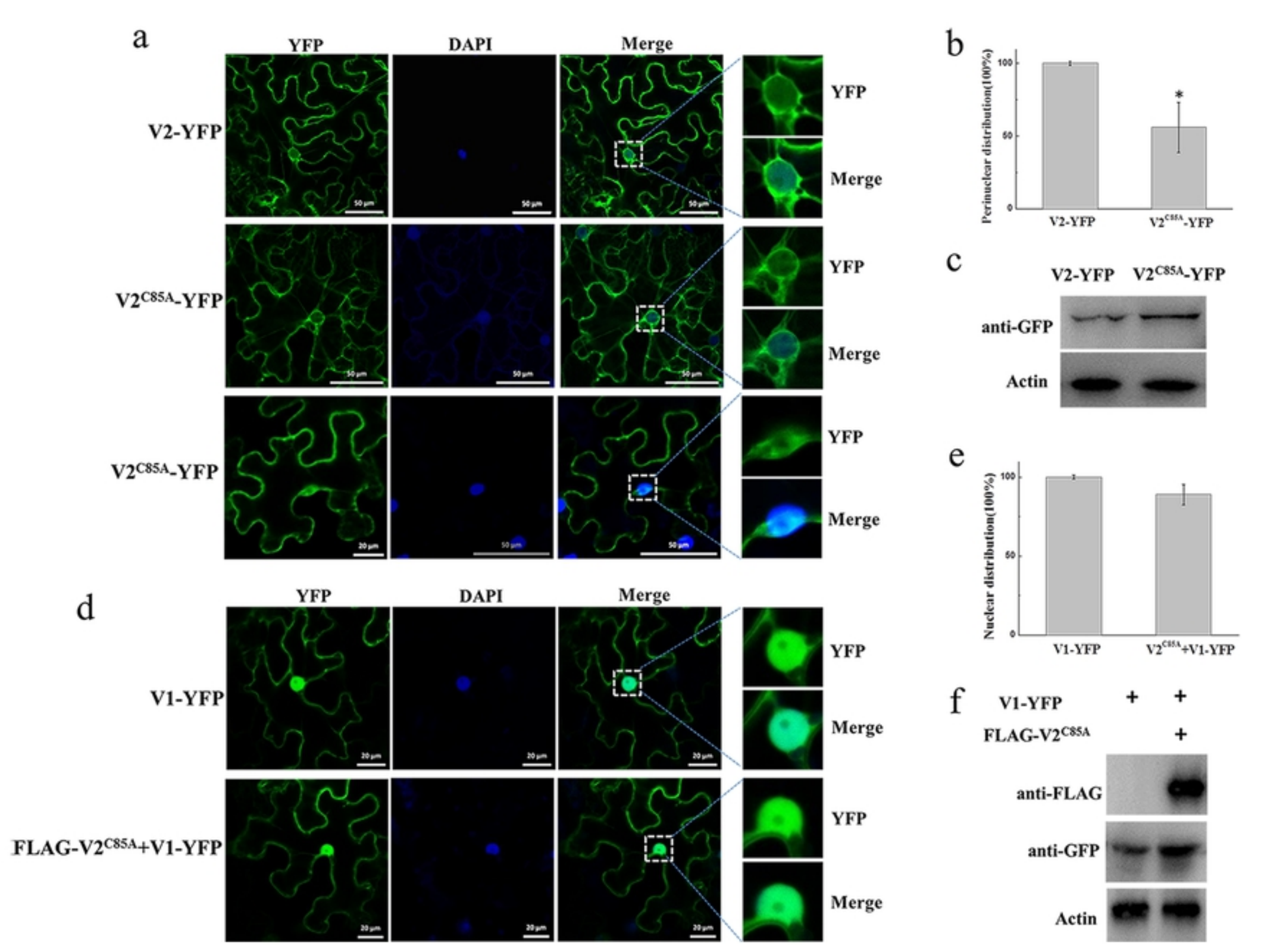
a
YFP
DAPI
Merge
V2-YFP
V2C85A-YFP
V2C85A-YFP
YFP
Merge
YFP
Merge
YFP
Merge
d
YFP
DAPI
Merge
V1-YFP
FLAG-V2C85A+V1-YFP
YFP
Merge
YFP
Merge
b
Perinuclear distribution(100%)
100
50
0
*
V2-YFP
V2C85A-YFP
c
V2-YFP
V2C85A-YFP
anti-GFP
Actin
e
Nuclear distribution(100%)
100
50
0
V1-YFP
V2C85A+V1-YFP
f
V1-YFP
+
+
FLAG-V2C85A
+
anti-FLAG
anti-GFP
Actin

Fig 5

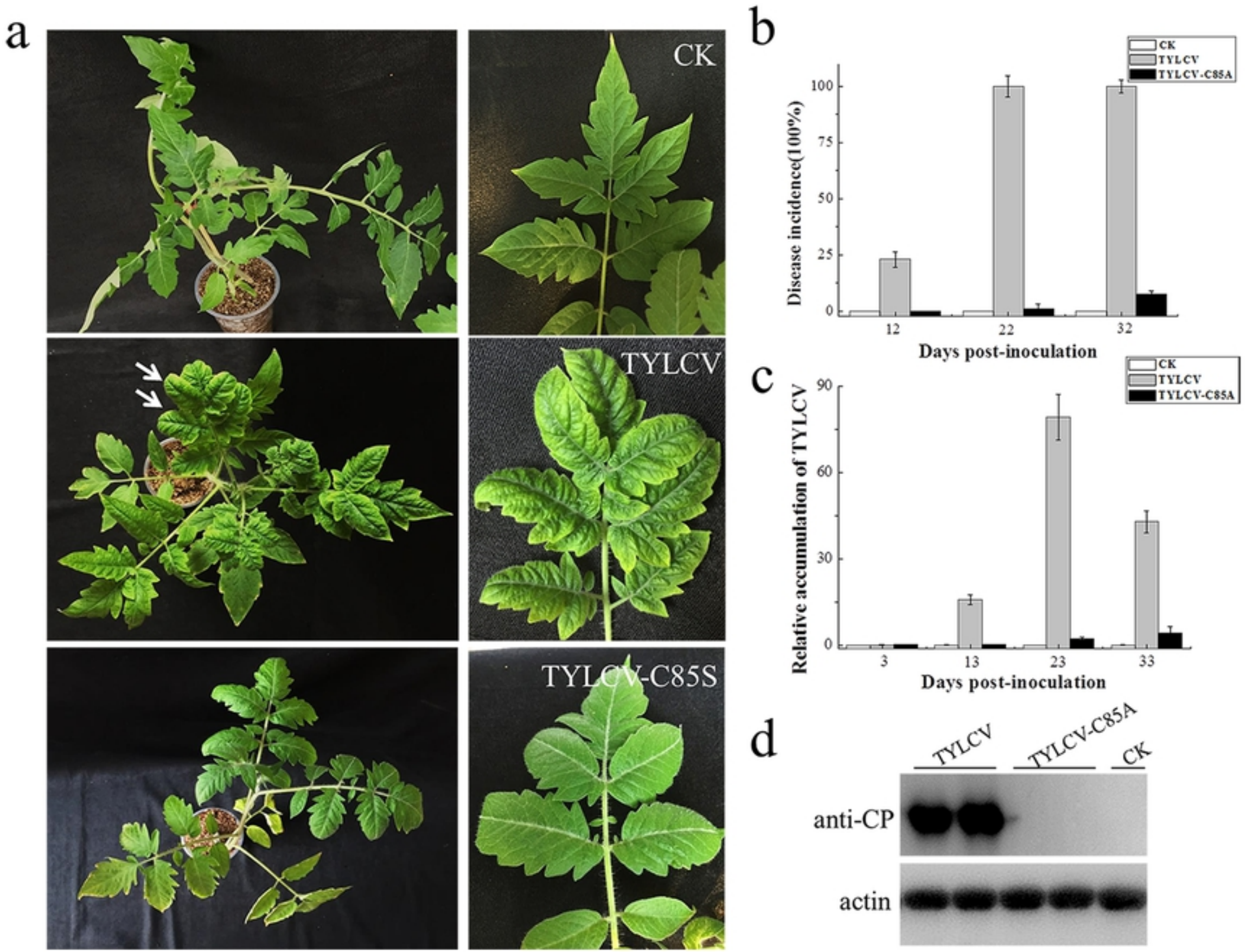
a
CK
TYLCV
TYLCV-C85S
b
CK
TYLCV
TYLCV-C85A
Disease incidence(100%)
100
75
50
25
0
12
22
32
Days post-inoculation
c
CK
TYLCV
TYLCV-C85A
Relative accumulation of TYLCV
90
60
30
0
3
13
23
33
Days post-inoculation
d
TYLCV
TYLCV-C85A
CK
anti-CP
actin

Fig 6

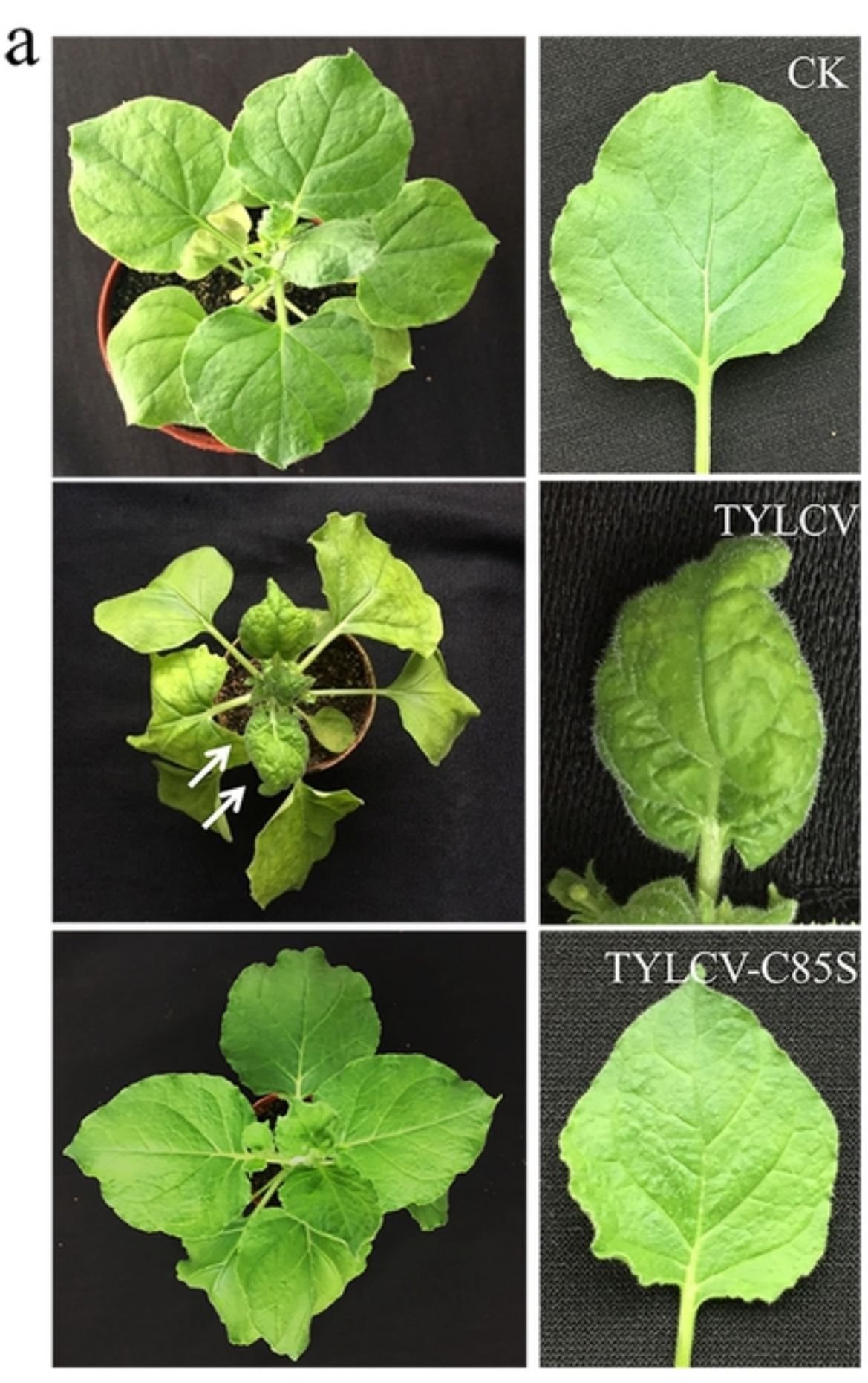
a
CK
TYLCV
TYLCV-C85S
b
CK
TYLCV
TYLCV-C85A
Disease incidence(100%)
100
75
50
25
0
12
22
32
Days post-inoculation
c
CK
TYLCV
TYLCV-C85A
Relative accumulation of TYLCV
480
360
240
120
0
3
13
23
33
Days post-inoculation
d
TYLCV
TYLCV-C85A
CK
anti-CP
actin

Fig 7

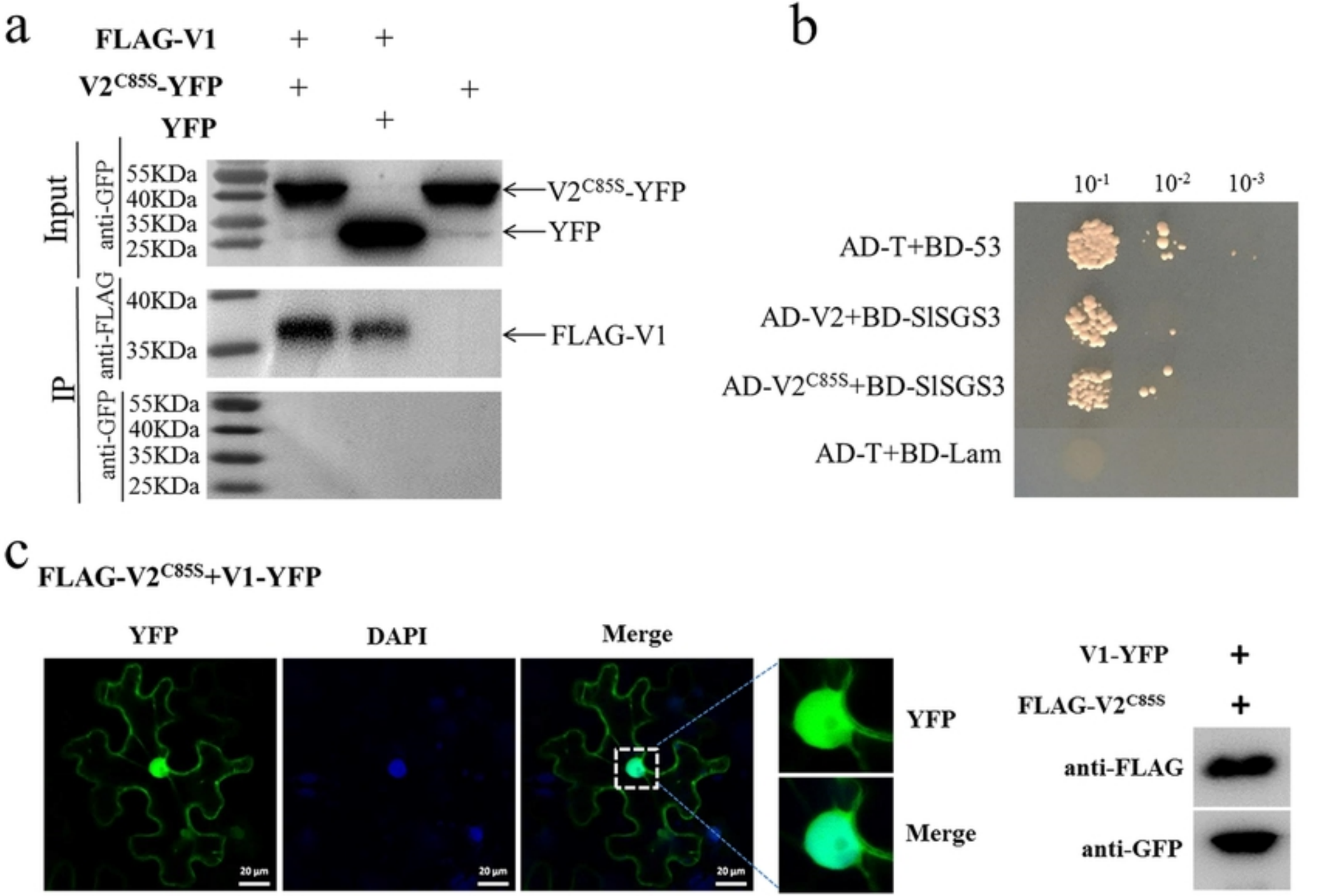
a
FLAG-V1 + +
V2C85S-YFP + +
YFP +
Input
anti-GFP
55KDa
40KDa
35KDa
25KDa
V2C85S-YFP
YFP
IP
anti-FLAG
40KDa
35KDa
FLAG-V1
anti-GFP
55KDa
40KDa
35KDa
25KDa
b
10-1 10-2 10-3
AD-T+BD-53
AD-V2+BD-SlSGS3
AD-V2C85S+BD-SlSGS3
AD-T+BD-Lam
c
FLAG-V2C85S+V1-YFP
YFP
DAPI
Merge
20 μm
YFP
Merge
V1-YFP +
FLAG-V2C85S +
anti-FLAG
anti-GFP

Fig S1